Chapter 1
Introduction to Pharmacometrics and Quantitative Pharmacology with an Emphasis on Physiologically Based Pharmacokinetics

Sherwin K. B. Sy, Xiaofeng Wang and Hartmut Derendorf

1.1 Introduction

Pharmacometrics has become a term that encompasses modeling and simulation for pharmacokinetics (PK), exposure–response relationship, and disease progression. Mechanistic models that describe the biochemical processes involved in a physiological system have become more utilized in drug development. The models of complex systems are generally classified as systems pharmacology. A quote from William Jusko describes the role of pharmacometrics in drug development: "Pharmacometrics lies at the heart of what drug companies do: collecting data from animals, normal volunteers, and patients; quantifying it, and then being able to determine what that data mean for optimizing drug efficacy and minimizing toxicity" (Nielsen and Friberg 2013). Pharmaceutical and biotech companies have invested heavily in establishing pharmacometrics expertise to utilize the preclinical, clinical, as well as human genomic data to understand the disease progression, the drug behavior, and its effect on individual patients and to personalize medicine to specific groups of patient population. The purpose of this chapter is to provide an overview of different approaches that were used in pharmacometrics in the context of pharmaceutical drug development.

H. Derendorf (✉)
Department of Pharmaceutics, College of Pharmacy, University of Florida, Gainesville, FL, USA
e-mail: hartmut@ufl.edu

S. K. B. Sy
Department of Pharmaceutics, University of Florida, Gainesville, FL, USA

X. Wang
Clinical Pharmacology, Otsuka Pharmaceuticals, Princeton, NJ, USA

S. Schmidt, H. Derendorf (eds.), *Applied Pharmacometrics,* AAPS Advances in the Pharmaceutical Sciences Series 14, DOI 10.1007/978-1-4939-1304-6_1

1.2 Classical PK Analysis

There are two primary approaches in the classical PK analysis: the compartmental modeling and the noncompartmental analysis. Compartmental modeling is based on the mass balance equations on the compartment and the noncompartmental modeling is based on the statistical moments derived from the time course of the drug concentration data.

Compartmental PK models are widely used to characterize the disposition of a drug using its concentration–time profiles sampled from body fluid such as plasma, serum, or whole blood following an administered dose. The general expression of the compartmental model is given in Eq. 1.1, where a series of exponential terms are used to fit to the drug concentration–time profile:

$$C(t) = \sum_{i}^{n} A_i e^{-\alpha_i t} \tag{1.1}$$

where i indicates each compartment, n is the total number of compartment, and A_i and α_i are called macroconstants reflecting the amount of the drug administered, the mass transfer between the compartments, and the elimination of the drug from the body. The number of compartments (n) determined by curve fitting is a rather abstract mathematical construct. The interpretation of Eq. 1.1 is that the body is a series of compartments; the drug is distributed between compartments, and is eliminated from the body. It was recognized that Eq. 1.1 was the solution of a series of ordinary differential equations derived by mass balance of each compartment.

The simplest compartmental model has one compartment with a bolus injection. The differential equation for the one-compartment model can be derived from mass balance; that is, the rate of change of the drug amount in the compartment equals the rate of the input minus the rate of output:

$$\frac{dVC}{dt} = rate\ of\ input - k_e VC, \quad \text{at } t = 0, C = C_0 \tag{1.2}$$

where V is the volume of the compartment, C is the drug concentration of the compartment, and k_e is the first-order elimination rate constant. C_0 is the initial condition of the differential equation, which is the drug concentration prior to drug administration. For a bolus injection, when using the delta function to represent the rate of input, the solution to the above equation, assuming V is a constant, is:

$$C(t) = \frac{Dose}{V} e^{-k_e t} \tag{1.3}$$

where $Dose$ is the input amount of the drug. Comparing Eq. 1.1 with Eq. 1.3, it is obvious that $A = Dose/V$, $\alpha = k_e$, and $n = 1$.

Because Eq. 1.1 is first-order kinetics, the half-life ($t_{1/2}$) can be estimated as $t_{1/2} = \frac{\ln(2)}{k_e}$. Keep in mind that only for first-order kinetics, the half-life is a constant. Equation 3 is often reparameterized to

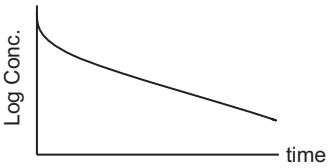

Fig. 1.1 Log concentration–time profile that follows a bi-exponential decline

$$C(t) = \frac{Dose}{V} e^{-\frac{CL}{V}t} \tag{1.4}$$

where $k_e = CL/V$ and CL refers to clearance. Clearance is one of the most important concepts introduced in PK. Additional information on clearance will be discussed in the section on the clearance definition.

In many cases, the disposition of a drug in the body follows a multi-exponential decline, which shows as multi-linear phases in the log concentration versus time profile shown in Fig. 1.1. This type of drug concentration profile is often characterized by two or more compartments. For a two-compartmental model with a bolus injection, Eq. 1.1 becomes

$$C(t) = Ae^{-\propto t} + Be^{-\propto t} \tag{1.5}$$

The half-life of the α phase and the β phase (or called the terminal phase) of the drug can be estimated as

$$t_{1/2,\alpha} = \frac{\ln(2)}{\alpha}, \quad t_{1/2,\beta} = \frac{\ln(2)}{\beta} \tag{1.6}$$

To estimate the overall half-life of a drug in the body following multi-exponential decline, the concept of "effective half-life" was introduced and the calculation is given in Eq. 1.7, e.g. for a two-compartment model:

$$effective\ t_{1/2} = \frac{1}{AUC}\left(\frac{A}{\alpha} t_{\frac{1}{2},\alpha} + \frac{B}{\beta} t_{\frac{1}{2},\beta}\right), \tag{1.7}$$

where AUC is the area under the concentration–time profile.

The differential equations for a two-compartmental model can be derived through mass balance on each compartment:

$$\begin{aligned} \frac{dA_c}{dt} &= Input\ rate - k_{12}A_c - k_e A_c + k_{21}A_p \\ \frac{dA_p}{dt} &= k_{12}A_c - k_{21}A_p \end{aligned} \tag{1.8}$$

where A_c and A_p refer to the drug amounts in the central and peripheral compartments, respectively; k_{12} and k_{21} are the mass transfer rate constants between the

central and the peripheral compartments, also called microconstants. The analytical solution to Eq. 1.8 for a bolus injection can be expressed in the same manner as Eq. 1.5, with the following micro- and macroconstant conversion:

$$\alpha + \beta = k_e + k_{12} + k_{21}$$

$$\alpha \times \beta = k_e \cdot k_{21}$$

$$A = \frac{Dose(\propto - k_{21})}{V_c(\propto - \beta)}$$

$$B = \frac{Dose(k_{21} - \beta)}{V_c(\propto - \beta)}.$$

Re-parameterization for a two-compartment model in terms of CL, intercompartmental clearance (Q), V_c, and V_p can be expressed as $k_e = \frac{CL}{V_c}$, $k_{12} = \frac{Q}{V_c}$, $k_{21} = \frac{Q}{V_p}$. For more detailed discussions of commonly used PK models including intravenous infusion and extravascular routes, the reader may refer to the textbooks on PK and pharmacodynamic (PD) analysis (Derendorf and Hochhaus 1995; Gabrielsson and Weiner 2000; Gibaldi and Perrier 1999; Rowland and Tozer 1989).

The compartmental models are often used to simulate concentration profiles from one dosing regimen to another, or from a single dose to a steady-state concentration profile. The compartmental model has its limitation, however. First, the number of compartments and the property of the compartments are rather abstract mathematical constructs. The underlying physiology of the model and the resulting model representation is subject to the analyst's interpretation. Second, the parameters do not have a clear physiological meaning, and so the source of the variability of the parameters cannot be clearly identified and be correlated to physiological reality.

A noncompartmental model is based on statistical moments of the concentration–time data (Dunne 1993; Yamaoka et al. 1978). The *n*th-order statistical moment has the following mathematical form:

$$\int_0^\infty t^n C(t) dt, \tag{1.9}$$

where t is time, n is the order of moment, and $C(t)$ is the drug concentration as a function of time. The area under the concentration–time curve (AUC), the moment curve (AUMC), and subsequently the mean residence time (MRT) can then be computed through integrating the concentration–time profile:

$$AUC = \int_0^\infty t^0 C(t) dt = \int_0^\infty C(t) dt \tag{1.10}$$

$$AUMC = \int_0^\infty t^1 C(t)dt = \int_0^\infty tC(t)dt \tag{1.11}$$

$$MRT = \frac{\int_0^\infty tC(t)dt}{\int_0^\infty C(t)dt} = \frac{AUMC}{AUC}. \tag{1.12}$$

In practice, the computations of the above parameters are carried out using numerical integrators such as the linear or log-linear trapezoidal rule on the discrete concentration–time data. PK parameters such as CL, V_{ss}, and $t_{1/2}$ can be derived from those statistical moments:

$$CL = \frac{Dose}{AUC} \tag{1.13}$$

$$V_{SS} = CL * MRT. \tag{1.14}$$

The terminal half-life can be calculated using the slope, λ_z, of the log concentration curve, $t_{1/2} = \frac{\ln(2)}{\lambda_z}$. If the concentration profile shows mono-exponential decline, the terminal half-life can also be calculated using the $t_{1/2} = \ln(2) * MRT$. If the concentration profile shows multi-exponential decline, the half-life calculated using $t_{1/2} = \ln(2) * MRT$ will be the "effective half-life," the same as the solution using Eq. 1.7 in the compartmental modeling approach. The underlying assumption of the noncompartmental modeling is that the PK of a drug is linear (Gibaldi and Perrier 1999). A special case is that the noncompartmental model is equivalent to a one-compartment PK model, where the PK parameters derived through noncompartmental analysis can also be obtained from a one-compartment model through integration of Eq. 1.2.

The advantage of a noncompartmental method compared to the compartmental model is that the results from the moment approach are less subjective on the analysts' bias of their model of choice (Yamaoka et al. 1978). From a numerical analysis point of view, noncompartmental analysis is using numerical integration over the time course of drug concentration to derive PK parameters rather than optimization on either algebraic or differential equations. Thus, the "noise" in the drug concentration–time profile has less impact on the PK parameters than that of compartmental modeling. For example, when calculating the effective half-life using Eq. 1.7, an unrealistically long effective half-life could be generated when the terminal phase slope cannot be accurately estimated. In that situation, the effective half-life estimated using $\ln(2) * MRT$ is more reliable. The noncompartmental analysis is often the choice for computing PK parameters of a drug for regulatory submission.

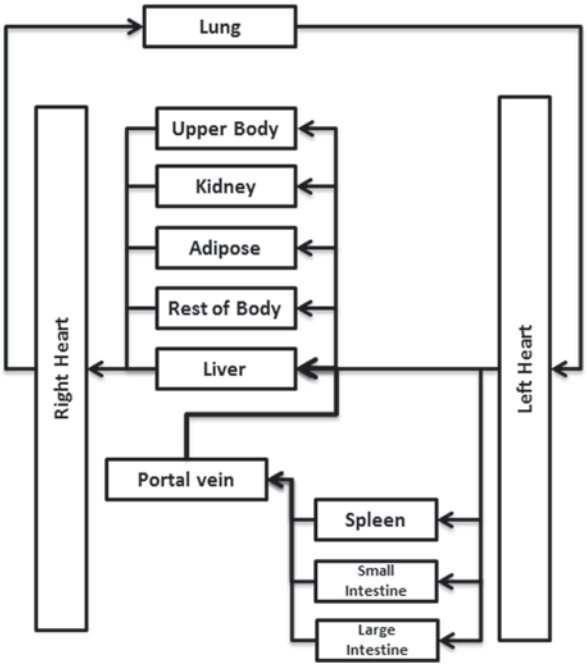

Fig. 1.2 An illustration of a PBPK model for a mammalian circulation system

1.3 Physiologically Based PK Modeling

The physiologically based pharmacokinetic (PBPK) model was developed to overcome the limitations of the compartmental modeling. The structure of the model, the property of the compartments, and the parameters are based on the underlying physiological and biological processes that are responsible for drug disposition.

1.3.1 History and Methodology of PBPK Approach

The concept of predicting the effect of a xenobiotic on a living organism based on mathematical models that incorporate real physiological parameters such as organ functions and flow rates was initially proposed by Teorell in (1937a, b). No progress was made in PBPK since Teorell's postulation of using mathematical models to describe xenobiotic disposition until the late 1950s, possibly due to the limitation in computational power. The most comprehensive development was made by Bellman and colleagues in the early 1960s (Bellman et al. 1963). The depiction of a PBPK model proposed by Bellman and his colleagues is shown in Fig. 1.2 with modifications. In the model, the tissue or lumped tissue was connected through blood flow. Blood flow through the main arteries and veins was assumed to be similar to a plug flow, that is, the drug concentration during the circulation was changing

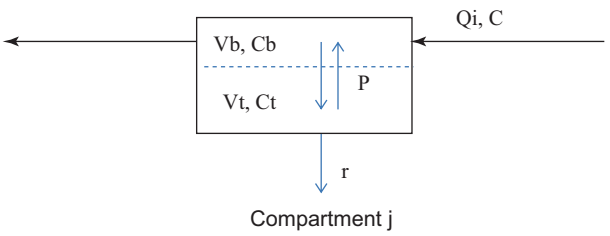

Fig. 1.3 A representative compartment with lumped interstitial and cellular regions

with time and longitude. The interstitial fluid and intracellular region were treated as perfectly mixed compartments. Based on those assumptions, the mathematical expression for the model was a set of difference-differential equations. The assumption of the plug flow leads to computational difficulties, as the entire past history of the drug concentration at each region of the body needs to be retained for the calculation of the successive time interval. Their work was discussed in detail and summarized by Bischoff and Brown in 1966 (Bischoff 1966). In the same publication, Bischoff and Brown discussed the application of mass transfer concept at great length at the levels of capillary, interstitial, and intracellular region. They also discussed the time needed for "mixed" drug concentration in the blood circulation versus the transient time of a typical human (~1 min). Based on the physiological reality and transport phenomena, the compartment property including the capillary, interstitial, and cellular region in Fig. 1.2 was characterized without accounting for every detail. They turned a set of difference-differential equations into differential equations such as Eqs. 1.15 and 1.16. Using a delta function to represent a bolus injection, the drug concentration profiles in different regions of the body were simulated.

To illustrate the mathematical expression and the parameters of a general PBPK model, for simplicity, if we assume that the interstitial and cellular regions are at equilibrium, a compartment in Fig. 1.2 can be illustrated as shown in Fig. 1.3. The differential equations describing the compartment were given in Eqs. 1.15 and 1.16:

$$\frac{V_{b,j}dC_{b,j}}{dt} = Q_j(C - C_{b,j}) - PA(C_{bf,j} - C_{tf,j}) \tag{1.15}$$

$$\frac{V_{t,j}dC_{t,j}}{dt} = PA(C_{bf,j} - C_{tf,j}) - r_j, \tag{1.16}$$

where Q_j is the blood flow rate for the j compartment, PA is the product of the membrane permeability and the membrane area; subscript b is for blood, t for tissue, and f for free drug concentration. The free and the total drug concentration can be correlated based on linear or nonlinear binding. The term r_j represents the elimination rate (metabolism and/or excretion) of the drug from compartment j; it can occur at different regions of the compartment. The drug can be administered through oral, intravenous, or intramuscular routes. The route of administration can be incorporated to the PBPK model.

As shown in Eqs. 1.15 and 1.16, there are three types of information required to solve a PBPK model: (1) the anatomy and physiology of a specific species; (2) the physicochemical properties, such as binding and membrane permeability, that are drug specific; (3) metabolism and excretion that are both drug- and species-specific. The anatomical and physiological parameters are usually available. Extensive data such as weight and blood flow rate through each tissue for different species were provided by Brown et al. (1997). However, physicochemical data and metabolism information are limited and often rely on *in vitro* studies or *in vivo* tests that were carried out in different species.

1.3.2 Number of Compartments in a PBPK Model

The two questions that an analyst needs to ask himself/herself when developing a PBPK model are: (1) how many compartments are needed and (2) how much detail is required for that compartment? Extensive work from a typical four-compartment model with flow-limited assumption with or without extensive details for a particular targeted organ to more than ten compartments describing the whole body can be found in the literature (Andersen et al. 1984, 1987; Bischoff et al. 1968, 1970, 1975; Liu et al. 2005; Peters 2008; Peters and Hultin 2008; Ramsey and Andersen 1984; Wang et al. 1997). A general consideration of the number of compartments to choose from and the details of the model depend on these information: the target organ, the physicochemical and pharmacologic properties of the drug that determine the drug transfer in the body, and the PK time scale (Bischoff 1975).

1.3.3 Target Organ

The structure of a PBPK model starts with the anatomy of the body. As the drug concentration in a target organ or at the site of action is of interest, single compartment is often used to represent the target organ. A significant amount of work using the PBPK approach has been done for anticancer drugs, central nervous system, hepatic metabolism and xenobiotic inhalation (Andersen et al. 1984, 1987; Baxter et al. 1994; Chen and Gross 1979; Collins and Dedrick 1983; Pang and Durk 2010; Ramsey and Andersen 1984; Reddy et al. 2005).

1.3.4 Mass Transfer Phenomenon

Lumping is often used for PBPK model reduction. There are two levels of lumping: (1) at the organ level and (2) at the cellular level. Lumping at the cellular level was originally discussed in details by Bischoff and Brown in their work mentioned above (Bischoff 1966). Lumping at the organ level was extensively discussed from

the late 1960s to the 1990s (Bischoff 1987; Bischoff and Dedrick 1968; Coxson and Bischoff 1987a, b; Gerlowski and Jain 1983; Nestorov et al. 1998). The basis for lumping is dependent on the mass transfer process and the physicochemical properties of a drug. The following section discusses the types of mass transfer function and the conditions for their applications.

1.3.4.1 Flow-Limited Assumption

The flow-limited assumption was made primarily due to the lack of information on membrane permeability. The criterion of flow limited was given as $\frac{PA_j}{Q_j} \gg 1$ (Bischoff 1975), that is, the membrane transfer is much faster than convection (from blood flow). Under this assumption, the free drug concentration in the tissue and in the blood is at equilibrium, $C_{tf,j} = C_{bf,j}$. Therefore,

$$C_{t,j} = C_{bf,j} + \frac{R_{\text{tot},j} C_{bf,j}}{K_{d,j} + C_{bf,j}}. \tag{1.17}$$

For linear binding, Eq. 1.16 can be simplified as $C_t = R * C_b$, where R is called the tissue to blood partition coefficient. Under flow-limited assumption, Eqs. 1.15 and 1.16 become

$$\left(V_{t,j} + \frac{V_{b,j}}{R_j}\right)\frac{dC_{t,j}}{dt} = Q_j\left(C - \frac{C_{t,j}}{R_j}\right) - r_j \tag{1.18}$$

Or if it is expressed using C_b, Eq. 1.18 becomes

$$(V_{b,j} + R_j V_{t,j})\frac{dC_{b,j}}{dt} = Q_j(C - C_{b,j}) - r_j \tag{1.19}$$

Equations 1.18 and 1.19 demonstrate that the concentration of a drug in a particular organ, $C_{b,j}$ or $C_{t,j}$, is determined by the value of $\frac{Q_j}{V_{b,j} + R_j V_{t,j}}$ and the elimination of that organ, $\frac{r_j}{V_{b,j} + R_j V_{t,j}}$. As such, lumping different organs or body regions depends on the blood flow rate through the organ, the partitioning of the drug between the blood and the tissue levels, and the elimination process of the organ (for an eliminating organ).

For noneliminating organs connected in parallel, the blood concentration entering those organs, C, is the same. Therefore, the blood concentration leaving the organ, $C_{b,j}$, and the concentration of the tissue, is determined by the ratio of $\frac{Q_j}{V_{b,j} + R_j V_{t,j}}$. The richly perfused organs with similar partition coefficient of the

drug are usually lumped into a single compartment. The blood flow rate through the compartment is $\sum_{j=1}^{n} Q_j$, and the volume of the compartment is $\sum_{j=1}^{n} V_{b,j} + R_j V_{t,j}$. The same principle can be applied to poorly perfused organs with similar partition coefficient. For a lipophilic compound, higher partition coefficient in the adipose versus the lean tissue resulted in different profiles of the concentration of the drug in the tissue, and therefore, a separate compartment for the lean tissue or the adipose tissue is often required. In addition, an organ or a body region with significantly low blood flow rate and low partition coefficient of the drug in those regions can be omitted in the PBPK model. Whether an eliminating organ can be lumped with a noneliminating organ depends on the ratio of the blood flow rate to the clearance of that organ (Bischoff 1975; Nestorov et al. 1998).

For organs that are connected in series, such as the venous–lung–artery channel or the splanchnic organs, the blood concentration profile leaving the channel and returning to the vein is determined by the organ that has the longest transient time, or the organ that eliminates the xenobiotics. If the partition coefficient between the plasma and the lung tissue is small, the transient time of the lung is much smaller than those of the vein and the artery. The vein and the artery often can be lumped to one compartment without including the lung, $V = V_{artery} + V_{vein}$, if the lung is not an eliminating organ. In the splanchnic channel, the splanchnic organs are often omitted, since the liver is the primary eliminating organ and the blood concentration leaving the channel is approximately represented by the liver. The gastrointestinal tract (GI) tract may be included to describe the absorption and/or reabsorption of the drug.

In general, a four-compartment lumped PBPK model, consisting of the blood compartment, the richly perfused compartment such as liver or kidney, the poorly perfused compartment such as the muscle, and a compartment representing the adipose tissue can adequately describe the drug disposition in the body. Other compartments may be added to describe the specific target organ as in the PBPK model to study tumor, wherein a separate compartment was incorporated to represent that organ where the tumor resides.

If the drug transfer across the membrane is fast enough compared to the mass transfer through convection (blood flow), the entire body can be modeled as a single-compartment model assuming that the blood concentration is at equilibrium with tissues at different regions. See the elimination-limited case below for the mathematical expression.

1.3.4.2 Membrane Limited

The opposite situation contrasting to the flow-limited mass transfer is the case wherein the membrane transfer is slow enough compared to the rate of the drug supply by blood flow, $\frac{PA_j}{Q_j} \ll 1$, so that the gradient of the drug concentration in the blood entering and leaving the compartment is negligible (Bischoff 1975). Therefore, $C_{b,j} \approx C$. Equations 1.15 and 1.16 for the compartment with membrane-limited transfer can be simplified as:

$$V_{t,j}\frac{dC_{t,j}}{dt} = PA(C - C_{tf,j}) - r_j. \tag{1.20}$$

If the drug transfer across the membrane of all regions of the body is slow enough that it can be considered negligible, the entire body can be modeled as a single-compartment model by only including the blood pool:

$$V_b\frac{dC}{dt} = Input - r_j. \tag{1.21}$$

1.3.4.3 Elimination Limited

In their publication on the general solution of a two-compartment model, Bischoff and Dedrick introduced the concept of the elimination-limited assumption, where the mass transfer is much more rapid than the total elimination rate (Bischoff et al. 1970). The importance of introducing the elimination-limited concept is to simplify a PBPK model to a one-compartment model. The criteria for when a system follows the elimination-limited profile is given in their study through a two-compartment open model under a flow-limited assumption, that is, the drug distribution to the tissue through the blood flow rate (mass transfer through convection) is much faster than the rate of elimination. In the elimination-limited situation, the entire body can be lumped into a one-compartment model:

$$\left(V_b + \sum_j^n R_j V_{tj}\right)\frac{dC_b}{dt} = Input - r_j. \tag{1.22}$$

Equation 1.21 has the same mathematical expression as the one-compartment model in classical compartmental modeling. The difference is that Eq. 1.5 derived from PBPK model gives the meaning to V_d, which is equivalent to $V_b + \sum_j^n R_j V_{t,j}$. In fact, the elimination-limited case does not necessary require flow-limited assumption. As long as the elimination rate is slow enough compared to both convection and membrane transfer, the elimination-limited case stands. This also explains why in covariate analysis in the population PK modeling, the volume of distribution often is related to body weight, as tissue volume is proportional to the body weight. The tissue concentration then can be easily calculated as $\frac{C_b}{R_{t,j}}$, where C_b is the blood concentration and $R_{t,j}$ is the partition coefficient of the organ. A typical example can be found for 2,3,7,8-tetrachlorodibenzo-*p*-dioxin (TCDD), since TCDD is known to remain in the biological system for a very long time. The half-life in human is around 5–10 years. Table 1.1 lists the physiological data for a standard human with body weight of 70 kg and the estimated value of $\frac{1}{\lambda}$ with $\lambda_i \approx \frac{Q_i}{k_{el}}\frac{V_{lip,b}}{V_b V_{lip}}$ for a

Table 1.1 Physiological parameters of TCDD for a standard 70-kg human

	Weight (kg)	Blood flow (L/day)	Partition coefficient	PA (mL/h)	Lipid content (kg)	$\frac{1}{\lambda}$
Lung	1.17	8064	6	Flow-limited	0.057	4.03×10^{-10}
Spleen	0.182	111	5	Flow-limited	0.0089	2.93×10^{-8}
Kidney	0.308	1786	6	9	0.015	3.49×10^{-7}
Adipose	14.994	374	100	30	12.9	1.08×10^{-7}
Liver	1.799	2088	6	731	0.088	4.45×10^{-9}
Skin	2.597	432	10	39	0.52	8.36×10^{-8}
Rest of the body	44.388	3273	1.5	98	2.84	3.31×10^{-8}

flow-limited case, or $\lambda_i \approx \frac{PA_i}{k_{el}} \frac{V_{lip,b}}{V_b V_{lip}}$ for a membrane-limited case, where the subscript lip refers to lipid content.

The lipid contents of each organ in Table 1.1 were calculated based upon the values from the literature (van der Molen et al. 1996). The elimination rate constant k_{el} was estimated conservatively assuming a half-life of 5 years. The values shown in Table 1.1 suggested that the elimination-limited assumption was satisfied for TCDD. This one-compartment model through PBPK reduction was adopted in human risk assessment in the environmental toxicology (Thomaseth and Salvan 1998; van der Molen et al. 1996).

1.3.5 PK Time Scale

The PK time scale plays an important role in PBPK model development (Bischoff 1975; Dedrick and Bischoff 1980; Nestorov et al. 1998; Oliver et al. 2001). For a standard male or female, the time it takes to complete one blood circulation is about 1 min. For most of the drug acting in the scale of several minutes, hours, days or longer, it can be assumed that the blood in the circulation is a uniform pool. However, more details are required in the model for the rapidly eliminated drug, in a time scale of minutes. The sampling site could also be important. The following example illustrates the methodology in the selection of the number of compartments to use for building a PBPK model for a short-acting drug.

1.3.6 Example 1: A PBPK Model for a Contrast Agent for Ultrasound Imaging

The PBPK model developed for a contrast agent for ultrasound imaging (Wang et al. in preparation) is shown in Fig. 1.4. The model has detailed information on the cardiovascular circulation and pulmonary circulation, which included the vena cava, right heart, pulmonary vein, lungs, pulmonary artery, left heart, and aorta. The actual sampling site and the administration site had to be specified in the model to

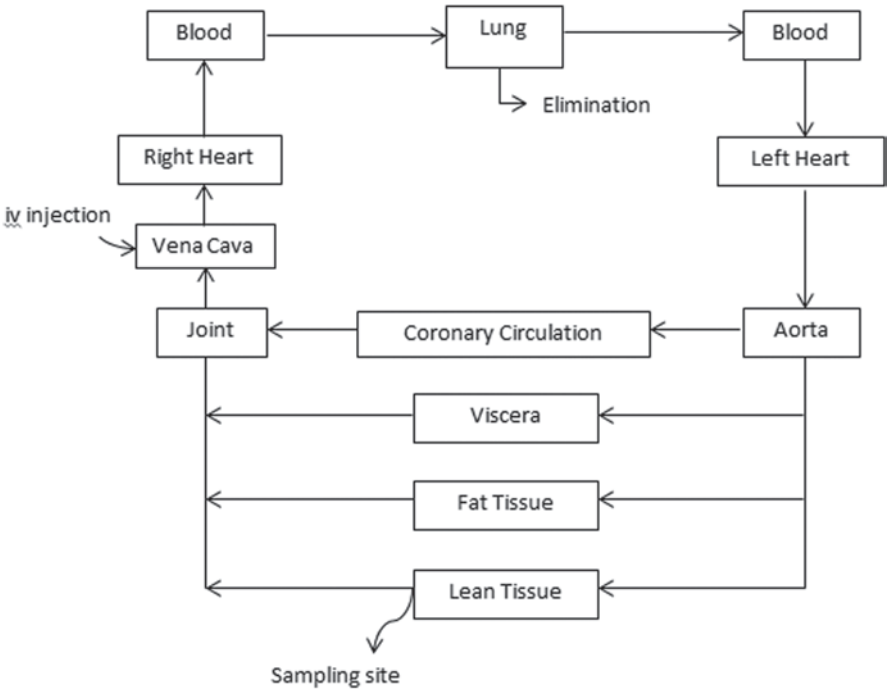

Fig. 1.4 Illustration of the PBPK model of the human body for a contrast agent used in ultrasound imaging

accurately describe the concentration of the agent in the blood circulation, the left and the right heart. Such detailed information became necessary due to the short time scale in its PK profile. For example, within 3 min following injection, blood concentration of the agent dropped tenfold. The left and the right sides of the heart are the target tissues for this contrasting agent. The lung is the eliminating organ. The adipose tissue and the lean tissue compartments were specified in the model, as the agent is a lipophilic compound. Coronary circulation was included in the model to evaluate whether coronary artery disease would have an impact on the PK of this agent. The viscera tissues consist of the kidney, the brain, the liver, etc. The blood flow rate per volume in these tissues is much faster than those of either adipose or lean tissues. Except for the lung, each compartment includes vascular and extravascular sub-compartments.

The lung is the primary eliminating organ for this compound. A heterogeneous compartment for the agent based on the anatomy of the lung and mass transfer is depicted in Fig. 1.5. As a static homogeneous lung compartment overpredicted the concentration in the alveolar gas phase during the absorption and under-predicted the concentrations during the elimination phase (Hutter et al. 1999), a heterogeneous lung model developed by Liguras and Bischoff (unpublished data), Frank (1982), and Bernards (1986) was adopted instead, as the one shown in Fig. 1.5.

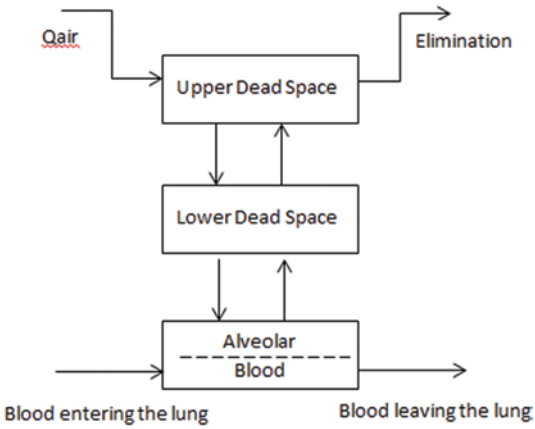

Fig. 1.5 Structure of the physiological model of the lung

The lung was modeled using three compartments based on the physiology of the lungs, consisting of an upper dead space plus a lower dead space in series and a perfectly mixed alveolar region. The dead space is taken to be that of the large bronchial vessels, such that there is no mass transfer between the air in the lung and the capillary blood. The volume of the alveolar compartment changes with inhalation and exhalation. The mass transfer between the air in the lung and the capillary blood occurs across the alveolar-capillary membrane. Mathematical equations describing the PBPK model including the lung compartment are given in Eqs. 1.23–1.32.

1.3.6.1 Whole-Body PBPK Model

For the left and right sides of the heart, and other compartments except the lung, the mass balance equations have the following form:

$$V_{b,j}\frac{dC_{tb,j}}{dt} = Q_j(C_a - C_{tb,j}), \tag{1.23}$$

where $V_{b,j}$ is the tissue blood volume, $C_{tb,j}$ refers to the concentration in the tissue blood, and C_a is the drug concentration in the blood entering the tissue. For other tissues, the mass balance equations take the form of a flow-limited case.

1.3.6.2 Lung Compartment

The breathing pattern is described by the following equation:

$$Q_{\text{air}} = 0.5 \cdot \omega\, TV \sin(\omega t), \tag{1.24}$$

where $Q_{\text{air}} > 0$ indicates an inhalation process, $Q_{\text{air}} < 0$ represents exhalation. In the following equations, all Q_{air} are absolute values, and the inhalation and exhalation

processes are identified by either a positive or a negative sign, respectively. The total dead space was modeled using two compartments.

For the upper dead space of the lung, the inhalation and exhalation processes were described by Eqs. 1.25 and 1.26, respectively, and the elimination rate for the lung was characterized by Eq. 1.27.

Inhalation:

$$V_{UPD}\frac{dC_{\mathrm{UPD}}}{dt} = -Q_{air}C_{UPD} \tag{1.25}$$

Exhalation:

$$V_{UPD}\frac{dC_{UPD}}{dt} = Q_{air}(C_{LPD} - C_{UPD}) \tag{1.26}$$

$$rex_{LU} = Q_{air}C_{UPD}. \tag{1.27}$$

For the lower dead space of the lung, the inhalation and exhalation processes were also described separately using Eqs. 1.28 and 1.29, respectively:

Inhalation:

$$V_{LWD}\frac{dC_{LWD}}{dt} = Q_{air}(C_{UPD} - C_{LWD}) \tag{1.28}$$

Exhalation:

$$V_{LWD}\frac{dC_{UPD}}{dt} = Q_{air}(C_{alv} - C_{LWD}). \tag{1.29}$$

For the alveolar region, the volume of the alveoli is described by a sinusoidal function, given that the volume of the alveoli changes with the breathing pattern:

$$V_{alv} = V_{alv,0} + 0.5 \cdot TV(1 - \cos(\omega t)). \tag{1.30}$$

And the corresponding inhalation process was characterized by coupled differential Eqs. 1.31 and 1.32:

$$\frac{dV_{alv}C_{alv}}{dt} = Q_{air}C_{LWD} + PA\left(C_{b,out} - \frac{C_{alv}}{P_{air}}\right) \tag{1.31}$$

$$V_{bLu}\frac{dC_{b,out}}{dt} = Q(C_{b,in} - C_{b,out}) - PA\left(C_{b,out} - \frac{C_{alv}}{P_{air}}\right). \tag{1.32}$$

The exhalation process was also defined by coupled differential Eqs. 1.33 and 1.34:

$$\frac{dV_{alv}C_{alv}}{dt} = -Q_{air}C_{alv} + PA\left(C_{b,\text{out}} - \frac{C_{alv}}{P_{air}}\right) \tag{1.33}$$

$$V_{bLu}\frac{dC_{b,out}}{dt} = Q(C_{b,in} - C_{b,out}) - PA\left(C_{b,out} - \frac{C_{alv}}{P_{\text{air}}}\right). \tag{1.34}$$

The breathing frequency is $\omega = 2\pi f$, where, f is the number of breaths/per minute. $V_{alv,0}$ is the functional residual capacity of alveoli; Q is the cardiac output; PA is the product of membrane permeability and area of membrane transfer. The subscripts refer to the following: UPD—upper dead space; LWD—lower dead space; alv—alveolar; b,in—blood entering the lung; b,out—blood leaving the lung; and V_{bLu} is the blood volume in the lung tissue.

1.3.7 Sensitivity Analysis in PBPK Modeling

As shown in the example above, there are several different types of parameters in a PBPK model. Parameter values for tissue volume, blood volume, and blood flow rates were obtained from published results (Brown et al. 1997). These values usually represent a typical male or female individual. Other parameters such as partition coefficient of a compound between blood and the tissue are often estimated based on *in vitro* or scaled-up studies from animals to human. The remaining unknown parameters are then estimated by fitting the model to the observed data. Given the large number of parameters, it is critical to evaluate the impact of the uncertainty of those parameters on the disposition of the compound in the body. This is often done through a local (derivative) and global (Monte Carlo method) sensitivity analysis. We used the first example to illustrate the importance of this analysis.

In Example 1, the anatomical and physiological parameters related to the lung such as the volume of the alveoli, the dead space inside the lung, the functional residual capacity, the tidal volume, and the breathing frequency were obtained from Guyton's textbook of physiology (Guyton and Hall 1996; Hall and Guyton 2011). The partition coefficient, $P_{\text{ft}} = C_{\text{fat}}/C_{\text{blood}}$, of 50, was estimated based on the oil/water partition ratio of the compound. According to the results reported for other lipophilic compounds such as dioxin or thiopental (Bischoff and Dedrick 1968; Wang et al. 1997), the partition coefficient for nonfatty tissue is approximately 10% of that of the fat tissue. Therefore, the partition coefficients of other nonfatty tissue were assumed to be $P_t = 5$. Table 1.2 listed the parameter values for a typical 70-kg healthy subject.

There are three remaining unknown parameters, the partition coefficient between air and blood, P_{air}, and the two permeability values, PA_{air} and PA_t. Both individual fitting and mean value fitting were conducted. Figs. 1.6 and 1.7 present the fitting of the mean values at 0.3 mg/kg dose level. The fitted parameter values are given below:

$$\text{PA}_{\text{air,}} = 42.0 \pm 4.2\ (\text{m}^3/\text{min})$$

$$\text{P}_{\text{air}} = \text{C}_{\text{gas}}/\text{C}_{\text{blood}} = 106 \pm 50.$$

Table 1.2 PBPK model parameters for a 70-kg healthy subject. (Parameter values from Guyton and Hall 1996)

Body weight = 70,000 g Male: cardiac output = 1.3 × Body weight$^{0.75}$ (mL/min) Coronary blood flow = 0.0455 × cardiac output (mL/min) Total blood volume = 6.3 L Blood volume in pulmonary circulation and cardiac circulation = 30 % of the total Blood volume Rest of the blood = 70 % of the total blood volume			
Blood volume in pulmonary circulation and cardiac circulation (mL)		*Parameters for the lung model*	
Pulmonary vein = 315 Lung capillary = 150 Pulmonary artery = 290 Right heart chamber = 340 Left heart chamber = 340 Vena cava = 340 Aorta = 100		Breathing frequency = 15 (No/min) Tidal volume (excluding dead space) = 350 mL Total dead space = 150 mL Upper dead space[a] = 50 mL Lower dead space[a] = 100 mL Functional residual capacity = 2300 mL	
Compartments[b]	*Tissue volume as fraction of body weight*[b]	*Tissue blood volume as fraction of the total blood volume*[b]	*Blood flow rate as fraction of cardiac output*[b]
Lung	0.0105	As shown above	1
Heart	0.0103		1
Viscera	0.05	0.0051/VBc	0.56
Adipose	0.214	0.0043/Vbc	0.065
Lean	Rest of the part	Rest of the part	Rest of the part

[a] Parameter values were obtained from Liguras and Bischoff (unpublished data), Frank (1982), and Bernards (1986)
[b] Values from Brown et al. (1997)

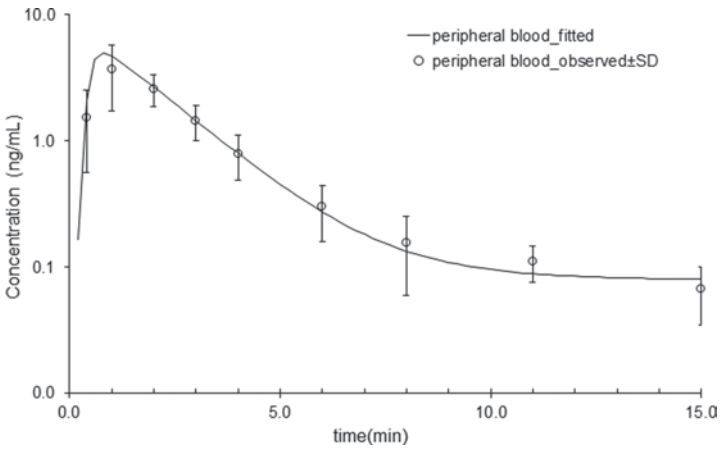

Fig. 1.6 Mean observed and fitted blood concentrations following bolus injection (dose of 0.3 mL/kg; *solid line* is model-fitted values, *symbols* are observed concentrations, *error bars* represent SD)

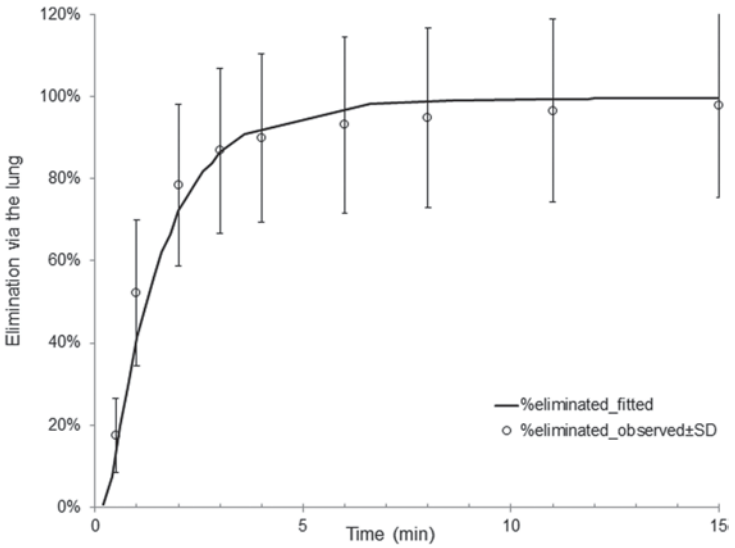

Fig. 1.7 Mean cumulative lung elimination (%) following bolus administration (dose of 0.3 mL/kg; *solid line* is model-fitted values, *symbols* are observed values of the elimination via the lung, *error bars* represent SD)

The ratio of PA to the blood flow rate through that tissue were such that

$PA_t/Q = 0.53 \pm 0.15$ (for the heart, the lung, and the viscera compartment)

$PA_t/Q = 1.80 \pm 0.22$ (for the lean compartment and the fat tissue).

To assess the impact of parameters on the PK of the agent, Monte Carlo simulation was conducted. The low, median, and high values of a parameter based on physiological reality were selected. For example, the total cardiac output range of 0.975–1.625 indicates that the low value of the total cardiac output is 0.975 with a median value of 1.3 and an upper range of 1.625. The results of Monte Carlo simulation demonstrated that only cardiac output, tidal volume of the lung and permeability have a significant impact on the concentration in the left heart of the agent. Other parameters such as the coronary blood flow rate, the fat content (though it is a lipophilic compound), the total blood volume, the breathing frequency, and functional residual volume have negligible effects on the concentration in the left heart. This analysis suggested that fixing a large number of parameter values using published data would have little impact on the fitted values of those three parameters (Table 1.3). This sensitivity analysis also provided information on potential source of interindividual variability.

1.3.8 Application of PBPK Modeling

There are many similarities in the anatomy and physiology of mammalian species; for example, many physiological processes vary as the 0.7–0.8 power of body weight and the anatomic variables are proportional to the body weight (Hu and

Table 1.3 Parameter effect of the contrasting agent disposition after sensitivity analysis

Parameters having significant effect	Parameters having negligible effect
Cardiac output (QTOTC)	Coronary blood flow rate (QCORC)
Permeability (PA)	Fraction of the fat (Wfc)
Tidal volume (TVC)	Total blood volume (VBTOTC)
	Breath No/min (BN)
	Functional residual volume (VAV0C)

Hayton 2001; Peters 1986; Savage et al. 2004; West et al. 1997, 1999). As such, the physiological process per unit body weight or organ weight tends to decrease as body size increases. Physicochemical parameters, such as blood-to-tissue partition coefficient and plasma protein binding, are not expected to have a great variation across species. Hence, a major application of PBPK model was in the field of species scaling (Boxenbaum 1982; Boxenbaum and Ronfeld 1983; Dedrick 1973; Dedrick and Bischoff 1980; Mordenti and Chappell 1989). One of the main limitations in the extrapolation of a PBPK model, from one species to another, is when significant difference in metabolic pathways and enzyme activities exist. Since the first PBPK model with flow-limited assumption for thiopental (Bischoff and Dedrick 1968), extensive application has been seen in drug development and environmental toxicology (Dedrick 1973; Peters 2012; Reddy et al. 2005; Rowland et al. 1973).

Peters presented a generic 14-compartment PBPK model that includes one compartment for the stomach, seven compartments to describe the absorption of a substance from the small intestine, and another compartment for the colon (Peters 2008). The dissolution of an orally administered substance from the GI tract is dependent on the product of the dissolution parameter and the difference between the solubility of the drug and its concentration. The model, being used for the *in vivo* prediction based on *in vitro* measurements, requires parameter for solubility, the pH of the buffer that was used for solubility measurement, and the in vitro absorption rate constant from Caco-2 permeability. For the estimation of drug concentration leaving a specific organ, the model utilizes plasma protein-binding information and tissue: plasma partition coefficients based on the work by Poulin and Theil (Poulin et al. 2001; Poulin and Theil 2000, 2002a, b; Theil et al. 2003). Peters used the model to predict the PK parameters of several compounds (Peters 2008; Peters and Hultin 2008). The measure to assess the quality of fitting was based on the reduced χ^2 -statistics and mean fold error. The author concluded that a "generic and integrative PBPK approach of drug disposition as a tool for a priori simulations and mechanistic evaluations of pharmacokinetics has the potential to improve the selection and optimization of new drug candidates" (Peters 2008).

In recent years, PBPK modeling has been applied to drug development and regulation (Zhao et al. 2009, 2011, 2012). A comprehensive review on the application of PBPK modeling in drug development and regulatory review/submission was provided in a number of articles from the Food and Drug Administration (FDA; Huang 2012; Huang and Rowland 2012; Leong et al. 2012; Rowland et al. 2011; Zhao et al. 2011, 2012). The articles summarized the major advances in the predictability of key PK parameters in human from *in vitro* data, the availability of dedicated

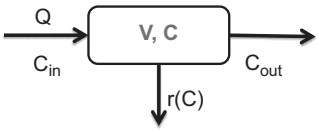

Fig. 1.8 Schematic representation of an eliminating organ

software platforms, and associated databases. Specific advances and contemporary challenges with respect to predicting the processes of drug absorption, distribution and clearance were reviewed, together with the ability to anticipate drug–drug interactions and the impact of age, genetics, diseases, and formulations on the PK of a drug. The value of this capability in selecting and designing appropriate clinical studies, its implications for cost-effective strategies, and a more holistic view of the application of PK across the preclinical and clinical drug development processes are considered. Finally, there is a greater focus on positioning PBPK within the drug development and approval paradigm, as well as its future application in personalized medicine.

1.4 Relationship Between Systemic and Tissue Clearance with PBPK Modeling Approach

1.4.1 Clearance Definition

Clearance is one of the most important concepts in PK. As Benet stated, "it allowed the field to develop a basic understanding and to make predictions as to how pathological and physiological changes would influence drug kinetics and drug dosing" (Benet 2010). By October 2009, there were more than 47,827 references found in PubMed under "drug clearance" (Benet 2010). The clearance concept was originally developed to quantify the functional efficiency of the kidney in the removal of urea (Grehant 1904a, b) and was then extended to describe the elimination of xenobiotics through the liver (Lewis 1948). Early contributions on developing the clearance concept for the whole body were made by Benet, Rowland, and Wilkinson (Benet and Galeazzi 1979; Rowland 1972; Rowland et al. 1973; Wilkinson 1987; Wilkinson and Shand 1975).

Using the definition provided by Wilkinson (1987), "the most general definition of clearance is that it is a proportionality constant describing the relationship between a substance's rate of transfer in amount per unit time, and its concentration, in an appropriate reference fluid." This is illustrated in Fig. 1.8 for an elimination organ.

The mathematical expression for clearance (CL) is given as follows:

$$CL = \frac{r(C)}{C_{in}}. \tag{1.35}$$

The extraction ratio reflecting the efficiency of an organ to remove a drug was defined as:

$$E = \frac{CL}{Q}, \tag{1.36}$$

where $r(C)$ is the elimination rate, C is the drug concentration inside the compartment, C_{in} is the drug concentration entering the organ, and Q is the blood flow rate through the organ.

The instantaneous clearance and extraction ratio from a blood or plasma concentration–time profile can be derived by applying mass balance to the eliminating organ, as in Fig. 1.8. Assuming that the organ is a homogeneous compartment such that $C_{out} = C$, where C_{out} is the drug concentration leaving the organ, the mass balance equation is then

$$V\frac{dC}{dt} = Q \cdot C_{in} - Q \cdot C - r(C) \tag{1.37}$$

given that $C = 0$ at $t = 0$.

By dividing Eq. 1.37 by $Q \cdot C_{in}$, the resulting expression is

$$\frac{V}{Q \cdot C_{in}}\frac{dC}{dt} = 1 - \frac{C}{C_{in}} - \frac{r(C)}{Q \cdot C_{in}}. \tag{1.38}$$

The third term on the right side of Eq. 1.38 is the definition of extraction ratio. The expression for instantaneous extraction ratio and clearance can be derived as follows:

$$E = 1 - \frac{C}{C_{in}} - \frac{V}{Q \cdot C_{in}}\frac{dC}{dt} \tag{1.39}$$

$$CL = Q\left(1 - \frac{C}{C_{in}}\right) - \frac{V}{C_{in}}\frac{dC}{dt} \tag{1.40}$$

Both Eqs. 1.39 and 1.40 show that, in general, instantaneous extraction ratio and organ clearance are time-dependent variables. Therefore, they have no definitive meaning unless the time when clearance is estimated is specified, or steady state is achieved.

At steady state, both C and C_{in} are constant, such that $\frac{dC}{dt} = 0$. The steady-state extraction ratio and clearance can be derived from Eqs. 1.39 and 1.40:

$$E_{ss} = 1 - \frac{C}{C_{in}} \tag{1.41}$$

$$CL_{ss} = Q\left(1 - \frac{C}{C_{in}}\right). \tag{1.42}$$

Since instantaneous clearance is of not much value for nonsteady-state situation, the mean clearance over time is more useful and can be derived by rearranging Eqs. 1.35 and 1.36 and integrating from 0 to infinity with respect to time:

$$\int_0^\infty E \cdot C_{in} dt = \int_0^\infty \frac{r(C)}{Q} dt$$

$$\int_0^\infty CL \cdot C_{\text{in}} dt = \int_0^\infty r(C) dt.$$

Applying the mean integration theorem to the equations above, there exists a value θ for clearance such that $\int_0^\infty CL \cdot C_{in} dt = \theta \int_0^\infty C_{in} dt$. The value θ is the mean clearance over time from 0 to infinity. Equations for the computation of mean clearance and mean extraction ratio are shown in Eqs. 1.43 and 1.44:

$$\overline{CL} = \frac{\int_0^\infty r(C) dt}{\int_0^\infty C_{in} dt} \tag{1.43}$$

$$\overline{E} = \frac{\int_0^\infty r(C) dt}{Q \int_0^\infty C_{in} dt}. \tag{1.44}$$

Using the example of an eliminating organ in Fig. 1.8, integration of the mass balance Eq. 1.37 from $t=0$ to infinity,

$$V \int_0^\infty dC = \int_0^\infty \left[Q \cdot C_{in} - Q \cdot C - r(C) \right] dt. \tag{1.45}$$

For limited dosage regimens, if $t \to \infty$, $C_{in} \to 0$ and therefore $C \to 0$. Together with the initial condition that $C = 0$ at $t = 0$, the left side of Eq. 1.45 is 0. Thus,

$$0 = \int_0^\infty \left[Q \cdot C_{in} - Q \cdot C - r(C) \right] dt. \tag{1.46}$$

By rearranging and dividing Eq. 1.46 by $\int_0^\infty Q \cdot C_{in} dt$, we obtain

$$\frac{\int_0^\infty r(C) dt}{\int_0^\infty Q \cdot C_{in} dt} = 1 - \frac{\int_0^\infty C \, dt}{\int_0^\infty C_{in} dt}. \tag{1.47}$$

The left side of Eq. 1.47 is the term for the mean extraction ratio (see Eq. 1.44). From Eq. 1.47, one can derive the relationship between mean extraction ratio and clearance:

$$\bar{E} = \frac{\overline{CL}}{Q} = 1 - \frac{\int_0^\infty C\,dt}{\int_0^\infty C_{in}\,dt} \tag{1.48}$$

$$\overline{CL} = Q\left(1 - \frac{\int_0^\infty C\,dt}{\int_0^\infty C_{in}\,dt}\right). \tag{1.49}$$

For an eliminating organ, $\int_0^\infty C\ dt < \int_0^\infty C_{in} dt$ holds true. One can deduce that the mean clearance is always smaller than the blood flow rate and the extraction ratio is smaller than one.

It has been observed that for some xenobiotics, the estimated extraction is greater than one, which is impossible as the amount of drug being removed cannot be greater than the amount supplied to the organ. Using the same eliminating organ shown in Fig. 1.8, if clearance is calculated using the blood samples leaving the specific organ, we would divide Eq. 1.46 by $\int_0^\infty Q \cdot C\ dt$, where C is the drug concentration in the blood stream leaving the elimination organ. Following the same steps to derive Eq. 1.48, we obtain Eq. 1.50:

$$\frac{\overline{CL}_{out}}{Q} = \frac{\int_0^\infty C_{in}\,dt}{\int_0^\infty C\,dt} - 1. \tag{1.50}$$

As one can see that for a high extraction drug, it is possible that $\frac{\int_0^\infty C_{in}\,dt}{\int_0^\infty C\,dt} - 1$ is greater than 1. And if $\frac{\int_0^\infty C_{in}\,dt}{\int_0^\infty C\,dt} - 1 > 1$, the extraction ratio defined in Eq. 1.48 is larger than 1, and the estimated clearance will exceed the blood flow rate. The conversion between $\overline{CL}_{\text{out}}$ and $\overline{CL}$ can be derived from Eqs. 1.48 and 1.50, such that

$$\frac{\overline{CL}}{Q} = \frac{\overline{CL}_{out}}{Q + \overline{CL}_{out}}, \tag{1.51}$$

where $\overline{CL}_{out}$ refers to the clearance computed from the blood samples taken from the blood leaving the organ and $\overline{CL}$ is the clearance estimated from the blood entering

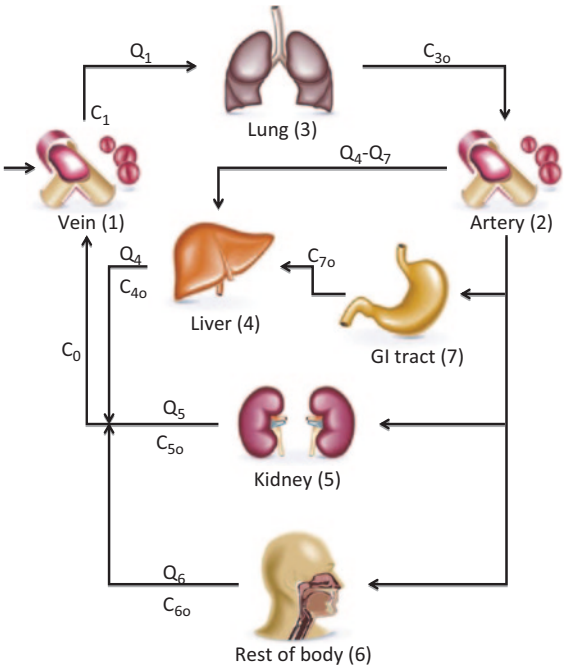

Fig. 1.9 A representative PBPK model used to illustrate total body clearance and organ clearance

the organ. The equation for extraction ratio, which is the left-hand side of Eq. 1.51, can be rearranged to obtain $\overline{CL}_{out}$ such that

$$\overline{CL}_{out} = \frac{\overline{CL}}{1-\overline{E}}. \tag{1.52}$$

We can extrapolate the result to total body clearance (TBC) in relation to cardiac output. The TBC, in this case, can also be greater than cardiac output for a compound that is rapidly eliminated through the lungs.

1.4.2 Establishing a General Relationship between TBC and Organ Clearance

It is often misunderstood that TBC is the sum of the individual organ clearance. The contribution of the organ clearance to the TBC depends on the anatomy of the body. In this section, we derived a general mathematical expression of the TBC with the individual organ clearance through PBPK modeling (Wang, Lam and Bischoff, unpublished work).

Figure 1.9 illustrates a representative PBPK model. This model consists of seven tissues, namely vein, artery, lung, GI tract, liver, kidney, and the rest of the body.

The first compartment C_1 represents the vein, second C_2 for the artery, third C_3 the lung, fourth C_4 the liver, fifth C_5 the kidney, sixth C_6 for the rest of the body, and seventh C_7 for the GI tract. In this example, an intravenous administration was utilized for the simplicity of the mathematical derivation. Assuming a flow-limited mass transfer, the equations representing the model based on mass balance are as shown in Eq. 1.53.

$$
\begin{aligned}
V_1 \frac{dC_{1(vein)}}{dt} &= Q_1 \cdot C_0 - Q_1 \cdot C_1 + K_I(t) \\
V_2 \frac{dC_{2(artery)}}{dt} &= Q_1 \cdot C_{3o} - Q_1 \cdot C_2 \\
V_3 \frac{dC_{3(lung)}}{dt} &= Q_1 \cdot C_1 - Q_1 \cdot C_{3o} - r_3(C_3) \\
V_4 \frac{dC_{4(liver)}}{dt} &= Q_7 \cdot C_{7o} + (Q_4 - Q_7) \cdot C_2 - Q_4 \cdot C_{4o} - r_4(C_4) \\
V_5 \frac{dC_{5(kidney)}}{dt} &= Q_5 \cdot C_2 - Q_5 \cdot C_{5o} - r_5(C_5) \\
V_6 \frac{dC_{6(rest\ of\ body)}}{dt} &= Q_6 \cdot C_2 - Q_6 \cdot C_{6o} \\
V_7 \frac{dC_{7(GI\ tract)}}{dt} &= Q_7 \cdot C_2 - Q_7 \cdot C_{7o} - r_7(C_7)
\end{aligned}
\tag{1.53}
$$

where $K_I(t)$ is the drug input function, $r_i(C_i)$ represents the rate of elimination from an eliminating organ, and the subscript o for out symbolizes the concentration leaving the organ. The initial conditions were assumed such that $C_i = 0$ at $t = 0$. The drug concentration at the joint point where the blood stream leaves the organ is represented by Eq. 1.54:

$$
Q_1 \cdot C_0 = Q_4 \cdot C_{4o} + Q_5 \cdot C_{5o} + Q_6 \cdot C_{6o}. \tag{1.54}
$$

Given the relationship above, we solve for the venous compartment C_1 (see Appendix for details), assuming that the input function $K_I(t) = 0$ and $C_i \to 0$ as $t \to \infty$:

$$
\begin{aligned}
&\int_0^\infty Q_1(C_1 - C_{3o})dt + \int_0^\infty Q_4(C_p - C_{4o})dt + \int_0^\infty Q_5(C_2 - C_{5o})dt \\
&\quad + \int_0^\infty Q_7(C_2 - C_{7o})dt = \int_0^\infty K_I(t)dt,
\end{aligned}
\tag{1.55}
$$

where $Q_4 \cdot C_p = Q_7 \cdot C_{7o} + (Q_4 - Q_7)C_2$.

Using Eq. 1.49 to compute the mean organ clearance, the generalized expression, except for the lung and liver, is shown in Eq. 1.56:

$$\overline{CL_i} = \frac{Q_i \int_0^\infty (C_2 - C_{io})dt}{\int_0^\infty C_2 dt} \in i \neq 3,4. \tag{1.56}$$

For the lung and liver compartments (C_3 and C_4), the resulting expressions for mean organ clearance are as follows:

$$\overline{CL_3} = \frac{Q_1 \int_0^\infty (C_1 - C_{3o})dt}{\int_0^\infty C_1 dt} \tag{1.57}$$

$$\overline{CL_4} = \frac{Q_4 \int_0^\infty (C_p - C_{4o})dt}{\int_0^\infty C_p dt}. \tag{1.58}$$

The total amount of drug elimination from the body, derived from solving the mass balance equations over the entire body, is $\int_0^\infty \sum_i r_i(t)dt = Q_1 \int_0^\infty (C_1 - C_0)dt = \int_0^\infty K_I(t)dt$. Following the expression in Eq. 1.43 for mean clearance, TBC or systemic clearance is derived as

$$\overline{CL}_{\text{total}} = \frac{Q_1 \int_0^\infty (C_1 - C_0)dt}{\int_0^\infty C_1 dt} = \frac{\int_0^\infty K_I(t)dt}{AUC} = \frac{Dose}{AUC}. \tag{1.59}$$

By substituting Eqs. 1.56–1.58 into Eq. 1.55, the relationship between TBC and organ clearance can be obtained as shown in Eq. 1.60 (see Appendix for derivation of Eq. 1.60):

$$\overline{CL_{total}} = \overline{CL_{lung}} + (1 - \bar{E}_{lung})\left[\overline{CL_{liver}} + (1 - \bar{E}_{liver})\overline{CL_{GI}} + \overline{CL_{kidney}}\right], \tag{1.60}$$

where $\bar{E}_i = \frac{\overline{CL_i}}{Q_i}$. A generalized relationship between TBC and organ clearance can then be established by extrapolating Eq. 1.60 to multiple eliminating organs:

$$\overline{CL_{systemic}} = \overline{CL_{lung}} + (1 - \bar{E}_{lung})\left[\overline{CL_{liver\_channel}} + \sum_i \overline{CL_i}\right], \tag{1.61}$$

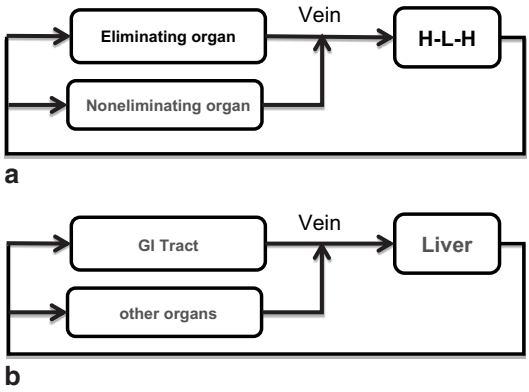

Fig. 1.10 Schematic illustration of **a** the left heart–lung–right heart (*H–L–H*) circulatory system and **b** the liver channel

where $\overline{CL}_{liver\_channel} = \overline{CL}_{liver} + (1-\bar{E}_{liver})\sum_j \overline{CL}_j$, and j indicates other organs except the liver in the liver channel. The subscript i in Eq. 1.61 includes all other body organs except the lungs and organs in the liver channel.

The mathematical equation in Eq. 1.61 is broadly applicable not only to the linear systems but also to the nonlinear systems because the assumption made in the derivation of Eq. 1.61 was flow-limited mass transfer. From Eq. 1.61, one can deduce that the contribution of organ clearance to the systemic clearance can be derived by following the circulation scheme starting from the arteries. For those organs connected in parallel, the contribution of organ clearance to systemic clearance is additive. For the organs connected in series, the contribution of the *i*th organ clearance to systemic clearance needs to be corrected by a factor of $(1-\bar{E}_{next\ organ})$. For example, following the blood circulation starting from the artery, the whole body can be viewed as consisting of two components connected in series, the rest of the body and the lung. Hence, in Eq. 1.61, the clearance of the portion that represents the rest of the body needs a correction factor of $(1-\bar{E}_{lung})$, as illustrated in Fig. 1.10a. The same is true for the liver channel such that the clearance of the GI tract or spleen also requires a correction factor $(1-\bar{E}_{liver})$, as represented in Fig. 1.10b.

The PBPK model used in this discussion is a lumped total body model but represents a rather general description of the anatomical structure of the mammalian system. The expression describing TBC and the individual organ clearances can be easily derived based on the location of the eliminating organ by following the circulation starting from the arteries. For these organs that are connected in series, the contribution of the first organ clearance to TBC equals $(1-\bar{E}_{i+1})\overline{CL}_i$, whereas for organs connected in parallel, the contribution of organ clearance to TBC is additive. Even though the current discussion only considered the example of an intravenous administration, the conclusions derived from this scenario are broadly applicable to other routes of administration.

1.5 Population PK

PBPK models provide the quantitative information between the dose and the concentration of the xenobiotic agent at different regions of the body. Interindividual variability in PK can be quantified based on the physiological/biological difference among the target population. However, it is often impractical to apply PBPK models directly to humans. The nonlinear mixed effect model (also commonly referred to as population PK) incorporating both fixed effect (identified covariates representing the known source of variability) and random effect (unidentified source of variability) was introduced in the 1970s by Sheiner et al. (1977). This approach adopts the simplicity of the classical PK models but correlates the PK parameters to covariates such as body weight, age, gender, etc. to quantify the source of variability in PK. For example, the volume of distribution is often correlated to the body size, and clearance to body weight, creatinine clearance, and enzyme activities. Covariate analysis is primarily performed through statistical analysis, together with the information on physiology, pathology, metabolism, and clinical relevance. The population PK modeling has been widely applied to the analysis of clinical PK data, especially to the sparse PK samples from phase 2/3 trials. With this approach, the source of variability in PK can be identified using large pooled datasets. More importantly, population PK modeling has innovated the drug development through model-based approach (Bhattaram et al. 2005). From what used to be an unusable sparsely sampled blood concentration from phase 2/3 trials, population PK modeling made it possible to identify the PK characteristics in patients based on their demographic information, metabolic status, liver/kidney function, and disease status to support labeling. This ability to hone into a specific factor responsible for drug response is what makes population PK a valuable tool for personalized medicine. In a survey from the US FDA between 2000 and 2004, they reported that pharmacometric analyses were pivotal in regulatory decision making in more than half of the 42 new drug applications (NDA; Bhattaram et al. 2005). In the case of a failed trial of nesiritide, they concluded that “dose selection based on pharmacometric analysis could have saved 3 years of drug development time and 1 clinical trial.”

1.5.1 Population PK Model Development

A population PK model consists of the structural model and the covariate models. The structural model takes the form of the classical compartment model to describe the concentration profile for a typical subject, whereas the covariate model quantifies the sources of intersubject variability: the known (covariates) and unknown (first level random effect term) source of variability (Sheiner and Ludden 1992; Sheiner et al. 1977). The second level of variability is within-subject variability that is often described by additive or proportional error model. Sometimes, a third level variability, called inter-occasion variability, is introduced to describe the variability for the same individual when replicate samples were taken following different dosing occasions.

Population PK model development and key considerations were clearly discussed in Meibohm et al. (2005) and regulatory documents (EMA 2007; FDA 1999), which include base model and covariate model development, internal and/or external model validation. The base model development follows the same principles as classical compartmental PK model development. Covariate model development and model validation will be described briefly in the following sections.

1.5.2 Covariate Models

Covariate models quantify the source of intersubject variability contributing to a PK parameter. For continuous covariates, the covariate model usually takes the form of a linear or power function, which probably originated from the allometric scaling concept. Different ways of parameterization of the covariate model are often done using the reference value of the covariate such as the median value, as shown in Eqs. 1.62 and 1.63:

$$TVP = \theta_0 + \sum_{i=1}^{m} \theta_i (Cov_i - Ref_i) \tag{1.62}$$

$$TVP = \theta_0 \prod_{i=1}^{m} \left(\frac{Cov_i}{Ref_i} \right)^{\theta_i} \tag{1.63}$$

where TVP is the typical value of a model parameter, Cov represents the covariates, m is the number of covariates, and θ_i is the coefficient.

For categorical covariates such as binary, ordered, or nonordered, an indicator function $I_i(Cov_i)$ is introduced such that if the covariate has a specific dummy variable value, a separate coefficient is designated:

$$TVP = \theta_0 + \sum_{i=1}^{m} \theta_i I_i (Cov_i) \tag{1.64}$$

$$TVP = \theta_0 \prod_{i=1}^{m} I_i (Cov_i)^{\theta_i} \tag{1.65}$$

and

$$I_i(Cov_i) = \begin{cases} 1, \text{if } i = i \\ 0, \text{otherwise} \end{cases} \tag{1.66}$$

Random effect is usually assumed to be log-normally or normally distributed, as given in Eq. 1.67, where n_j follows a normal distribution with mean 0 and covariance matrix Ω:

$$P_j = TVP \times \exp(\eta_j) \quad \text{or} \quad P_j = TVP + \eta_j. \tag{1.67}$$

1.5.2.1 Allometric Scaling

One of the approaches for covariate model development is by applying allometric scaling principle. Thus, the body weight often contributes to clearance to the power of 0.75 and to the volume of distribution to the power of 1. The allometric scaling is also often used for scaling PK parameters obtained from the adult to the pediatric population.

1.5.2.2 Stepwise Regression

Stepwise regression is a common statistical method used in covariate model building. The algorithm includes forward addition, backward elimination, or combination of forward addition and backward deletion in stepwise fashion. This process is automated in Perl-Speaks-NONMEM. Each step of the model building process in the forward inclusion involves testing the effect of each covariate on the appropriate model parameter in a separate model run, such that the statistical significance of each covariate–parameter relationship is screened individually (univariate analysis). Covariates that reduce the objective function above a predefined significance level are added to the PK model. The backward elimination step starts with the final model from the forward inclusion step; the subsequent removal of each covariate is also based on a predefined difference in the objective function. The hypothesis testing to discriminate alternative hierarchical models is based on the likelihood ratio test, often at preset *p*-values for the forward inclusion and backward elimination of, e.g., 0.05 and 0.01, respectively. The differences in the objective function values of two alternative models is equivalent to −2 log-likelihood, which follows a chi-squared distribution with *n* degrees of freedom, where *n* is the difference in the number of parameters in the hierarchical models. A difference of 3.84 and 6.64, for example, in the value of the objective function is considered significant under the likelihood-ratio test for $n = 1$ and *p*-values of 0.05 and 0.01, respectively.

1.5.2.3 Full Covariate Model

Because covariates often have collinearity and depending on the degree of correlation between covariates, the statistical inference approach such as stepwise methods could include a covariate that is not preferential. An algorithm of using full covariate model approach was proposed as an alternative for covariate model building (Agoram et al. 2006; Ravva et al. 2009). The decision on which covariate to include is based on exploratory graphics, scientific and clinical interest, mechanistic plausibility, or previous knowledge of these relationships. Covariates that are both statistically insignificant and clinically irrelevant can be dropped during covariate model development. The inferences on which covariate has clinical importance are then based on the magnitude of the estimated effect and the precision (Agoram et al. 2006). This approach is a simplification of the global model approach (Burnham

and Anderson 2002) and is claimed to be the preferred choice when the goal is to estimate the magnitude of an effect (Harrell 2001). A hybrid approach can also be implemented, starting with a full covariate model from which covariates are tested using stepwise backward deletion.

1.5.2.4 Case Deletion to Determine Influential Individual

The statistical inferences based on maximum likelihood or likelihood ratio test are easily influenced by outliers or a few individuals (not necessarily outliers) in the data. Influential individual or a group of influential individuals can be evaluated using case-deletion diagnostics. The jackknife method evaluates how removing a specific individual affects the objective function values of the base model and the one with covariate, both models with all the data versus the one with the specific individual removed (Sadray et al. 1999):

$$\Delta OFV_{jackknife,i} = (OFV_{final,n} - OFV_{basic,n}) - (OFV_{final,n-1} - OFV_{basic,n-1}). \quad (1.68)$$

The algorithm fits both the covariate model and the base model to the dataset containing all the individuals and the dataset with the specific individual removed. The $\Delta OFV_{jackknife,i}$ value in Eq. 1.72 is obtained for each individual of the dataset. The "shark" plot with the number of subjects removed on the *x*-axis and the change in OFV on the *y*-axis and curves showing both positive and negative ΔOFV_i can be used as visual inspection for case-deletion diagnostics.

1.5.2.5 Covariate Identification Through PBPK Modeling

As mentioned in the section of PBPK modeling, lumping has been used to simplify the complicity of a PBPK model without losing the key physiological reality of the model. During the lumping process, covariates having impact on the PK can be identified. This approach requires a PBPK model that can be developed using preclinical data. Sensitivity analysis of the PBPK model can also assist in identifying the factors that could have significant impact on the disposition of a xenobiotic.

The example below demonstrating the advantage of using PBPK modeling to identify the covariate was from a collaboration between Bischoff and Stanski in the early 1990s (Bischoff 1992). It was observed that the amount of thiopental needed to be administered to elderly patients (about 70–80 years old) was much less than that used for a standard 30-year-old healthy male. Therefore, age could be considered as a covariate for dose adjustment for thiopental based on the classical PK and population PK models. To investigate the age effect on thiopental PK, a PBPK model (Bischoff and Dedrick 1968) was applied to the PK data obtained from clinical studies. An adipose tissue compartment was included in the PBPK model for thiopental, as this compound is highly lipophilic. The differences in cardiac outputs between young adult subjects at 30 years of age versus the geriatric patients at 70 years

were taken into account in the PBPK model. By incorporating the physiological difference in cardiac output between the two age groups, the PBPK model captured well the difference in the exposure of thiopental for patients at age 30 versus those at 70 years, without having to incorporate age as a covariate of the model. This work was continued by Wada and colleagues to demonstrate the underlying mechanism behind the observed age effect in thiopental PK (Wada et al. 1997). Their results showed that the difference were due to the decline in cardiac output, followed by the increase in fat content with age. Since the cardiac output starts to decline at approximately 40 years of age, a nonlinear covariate equation to link clearance with age would be necessary. However, using the known data of age and gender differences in cardiac output and BMI (Brandfonbrener et al. 1955; Freedson et al. 1979; Guyton and Hall 1996), the change in clearance and volume of distribution of thiopental with age can be derived from these relationships.

1.5.2.6 Clinical Relevance in Covariate Model Development

Clinical relevance is a key consideration in covariate model assessment. In general, if the contribution of a covariate to the PK parameters resulted in less than 20% difference in systemic exposure using the bioequivalence (BE) criteria, this covariate can be ignored or dropped even though it is shown to be statistically significant. Sometimes, if a drug has a large therapeutic window and the influential covariate determined from the PK analysis does not have any significant impact on clinical endpoints, this covariate can be removed. In contrasting situations, the lack of statistical significance does not necessarily indicate that the covariate tested is lacking impact on the clinical endpoints. For example, due to limited sample size (< 10% of the subjects with a specific co-medication) or limited range of the covariate tested such as age, the impact of co-medication or age effect on the PK may not be statistically significant.

1.5.2.7 Power and Sample Size Calculation

Sample size (the total number of subjects and the sampling time per subject) is critical for population PK development. To be able to detect the interindividual and intraindividual variability, a minimum of two PK samples per subject is necessary. Ogungbenro and Aaron have demonstrated the minimal samples size requirement for a one- or two-compartmental PK model (Ogungbenro and Aarons 2008) based on the confidence interval of the PK parameters estimated.

Another statistical methodology called the Monte Carlo Mapped Power (MCMP) to determine the power and sample size calculation for covariate model development was introduced by Vong et al. (2012). Using the difference in individual's objective function values between the reduced and full models ($\Delta iOFV = iOFV_{reduced} - iOFV_{full}$), the MCMP analysis tests for drug or covariate effect by the summation of the individual's contribution to the overall objective

function value in the likelihood ratio test (Vong et al. 2012). The MCMP uses the sum of the n $\Delta iOFV$ instead of the overall ΔOFV to base its statistical inference. The algorithm maps the statistical power over a specified sample size range. The MCMP method is simple to run without the need for correcting for type I error that is associated with stochastic simulations and estimations (Ette et al. 1998; Kowalski and Hutmacher 2001; Lee 2001).

1.5.2.8 Model Evaluation

Model evaluation is a key step in population PK model development. Diagnostic plots, bootstrap, shrinkage in the η (Savic and Karlsson 2009), prediction-corrected visual predictive check, internal validation through dataset split are often used to evaluate the model. In addition to those approaches, external validation with additional datasets is a preferable method when feasible.

1.5.3 Application of Population PK Model

Since Sheiner's first and subsequent publications that established the population PK model methodology, population PK modeling and simulation together with information on disease progression, placebo response, dropout rates, as well as exposure–response (ER) of drug treatment, have been used in regulatory decision making, clinical trial waiver, as well as identification of design flaws and trial implementation problems prior to running a trial. These strategies have shown to decrease costs, improve the likelihood of achieving the trial goals, and generate conclusive findings (Brindley and Dunn 2009; Holford et al. 2010). Kimko and Peck recently edited a textbook on clinical trial simulation that encompasses diverse areas relevant to drug development such as metabolic disease, cardiovascular, infectious disease, oncology, and many other fields (Kimko and Peck 2011).

Yang et al. took an approach of incorporating a case–control comparison in the ER analysis to reduce the bias introduced by confounding risk factors when evaluating the recommended dosing regimen for trastuzumab in a registration trial (Yang et al. 2012). Their analysis suggested that patients with the lowest quartile of trastuzumab exposure did not benefit from addition of trastuzumab treatment to chemotherapy. However, contrary to the nonresponder hypothesis for this subgroup with the lowest quartile of tratuzumab, this subgroup appeared to be more sensitive to a higher trastuzumab exposure than the remaining 75 % population, suggesting that increasing trastuzumab exposure in the low-exposure subgroup may result in better overall survival (OS) benefit. This analysis justified the FDA recommendation of conducting postmarketing clinical trials to investigate a dosing regimen with higher exposure and acceptable safety in the identified subgroup and to prospectively evaluate whether this regime will result in acceptable OS benefit.

Other examples can be found from the approval of the 0.8 mg/kg once-weekly regimen of etanerceptin pediatric patients with juvenile rheumatoid arthritis. The clinical trial simulation confirmed that the 0.8 mg/kg once weekly yielded overlapping steady-state time–concentration profiles with that of 0.4 mg/kg SC twice weekly, leading to equivalent clinical outcomes (Yim et al. 2005).

The author (Wang) utilized model-based approach to apply for waiver of clinical pharmacology trial for a novel tyrosine kinases inhibitor that was under development in oncology. The absolute bioavailability of the tablet was required in the NDA submission. However, to conduct a clinical trial to obtain the absolute bioavailability was difficult, since the intravenous dosage formulation needed to be developed, and the study can only be conducted in cancer patients due to genotoxicity. A population PK model of the PK datasets obtained from several phase I dose escalation trials with either oral solution or tablet was developed with the formulation as one of the covariates. Covariate model test demonstrated that the formulation was not a statistically significant covariate. The health authority accepted this approach and a standalone absolute bioavailability trial was no longer required. The example listed above demonstrates how the model-based approach can cut development costs, as well as improve trial designs to come to conclusive findings.

1.6 PD Models for Continuous Response Variables

PD often refers to as the body's response to drug. Derendorf et al. defined PD as "a broad term that is intended to include all pharmacological actions, pathophysiological effects and therapeutic responses, both beneficial and adverse, of an active drug ingredient, therapeutic moiety, and/or its metabolite(s) on the various systems of the body from subcellular effects to clinical outcomes. Pharmacodynamic studies can provide information about a drug's mechanism of action or about its dose-response relationship where response can be expressed as a direct or indirect measure of efficacy and/or safety of the drug" (Derendorf et al. 2000). As collecting biomarker information is becoming common in clinical trials, modeling the exposure and biomarker responses has become critical in model-based drug development.

PK/PD studies intend to link the dose–exposure profile relationship with the PD response, in particular, the time course of the pharmacological/pathophysiological effects (Derendorf et al. 2000). Integrated PKPD models are categorized according to the manner in which the PK and PD data are related. The two types of basic PD models that are often used to establish PKPD relationships are the direct and indirect response models. Based on receptor theory, the response of a drug is triggered by the free drug concentration at the site of action. Since the systemic blood or plasma drug concentration samples were collected during a trial, while the effect or response is dependent on the concentration at the effect site, a delay in response might be observed when linking the blood/plasma concentration to the drug response. If the effect is further downstream in the process, a longer delay in response could be observed.

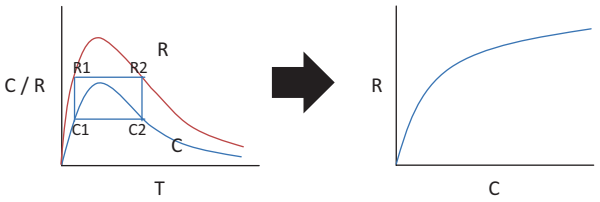

Fig. 1.11 Relationship between drug concentration and response in a direct response relationship

1.6.1 Direct response PD Model

In the direct response model, the linear, E_{max}, or sigmoidal E_{max} models are often used. Equation 1.69 is the expression for the sigmoidal E_{max} model. When γ equals 1, it is the called the E_{max} model:

$$E(C) = E_0 \pm \frac{E_{max} C(t)^{\gamma}}{EC_{50}^{\gamma} + C(t)^{\gamma}}, \tag{1.69}$$

where E_0 is the baseline of the response and E_{max} is the maximum response. C is the concentration of drug and $C(t) = \frac{\text{Dose}}{V} e^{-\frac{CL}{V}t}$ is the drug concentration at which 50% of the maximum response is achieved and γ is the sigmoidicity factor that determines the steepness in the linear portion of the curve. The direct response relationship assumes that the processes involved in the drug transfer to the site of action and eliciting the response is rapid enough compared to the disposition of a drug. Thus, for the same drug concentration, the response elicited by the drug is the same, regardless of the time to reach that drug concentration. As shown in the left panel of Fig. 1.11, the concentration $C1$ in the ascending phase of the concentration–time profile with the equivalent concentration level at $C2$ in the descending phase has a corresponding response $R1$ in the ascending phase of the response profile and the equivalent response level $R2$ in the descending phase. In other words, there is only one value for the response corresponding to one value for the drug concentration, as shown in the right panel of Fig. 1.11.

1.6.2 Indirect Response Model

It is often the case in pharmacology that the effect of the pharmacological agent is lagging behind the drug concentration–time course, where, the response versus concentration does not exhibit a one-to-one relationship, often called a hysteresis loop (counterclockwise hysteresis), as shown in the right panel of Fig. 1.12. The temporal dissociation between the time courses of drug concentration and effect results in the hysteresis pattern and is likely caused by a distributional delay between the drug concentrations in the plasma and the effect site (Derendorf et al. 2000).

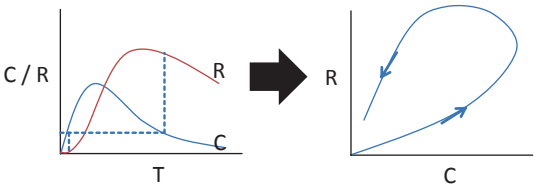

Fig. 1.12 Relationship between drug concentration and response in an indirect response relationship

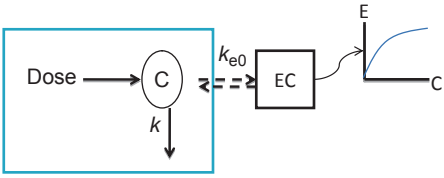

Fig. 1.13 Schematic representation of the effect compartment linking to a pharmacodynamic model

The two different approaches often used to describe the observed delay in the plasma concentration and drug response are the effect compartment model originally proposed by Sheiner et al. (1979) and the indirect response model with differential equation by Jusko (Dayneka et al. 1993; Jusko and Ko 1994).

1.6.2.1 Effect-Compartment PD Model

The effect-compartment model links the drug effect to the drug concentration of a hypothetical effect compartment (Sheiner et al. 1979), instead of the drug concentration in the systemic circulation. In the effect-compartment model, it was assumed that the drug amount entering the effect compartment is negligible, so that the plasma concentration of the central compartment can be described without the mass transfer between the central compartment and the effect compartment. The drug concentration in the effect compartment is at equilibrium with that of the central compartment. The equilibration process between the plasma drug concentration and the effect site is determined by the first-order rate constant k_{e0} that also describes the loss of drug from the effect compartment (Derendorf et al. 2000). The illustration in Fig. 1.13 shows a schematic representation of the link model, where EC refers to the effect compartment. When the drug response links to the drug concentration of the effect compartment, the hysteresis observed will be collapsed.

Equations for calculating the effect compartment concentration can be found in Gabrielsson and Weiner (2000). For example, for a one-compartment model with bolus injection, the plasma concentration can be calculated using Eq. 1.4, and the effect compartment concentration can be expresses as:

$$C_e = \frac{Dose \cdot k_{e0}}{V_e\left(k_{e0} - \frac{CL}{V}\right)}\left(\exp\left(-\frac{CL}{V}\cdot t\right) - \exp(-k_{e0}\cdot t)\right), \tag{1.70}$$

where C_e is the drug concentration in the effect compartment, V_e is the volume of the effect compartment.

1.6.2.2 Indirect Response Models

The indirect response models was developed based on the receptor theory and signal transduction, where a series of delay could occur during those processes caused by indirect-response mechanism such as a synthesis or dissipation of an endogenous substance or response mediator. Dayneka et al. proposed four basic models for indirect PD response (Dayneka et al. 1993; Jusko and Ko 1994). The generalized form of the indirect response models in the absence of drug is described as follows:

$$\frac{dR}{dt} = k_{in} - k_{out}R, \tag{1.71}$$

where k_{in} is the zero-order constant for the production of the response, and k_{out} refers to the first-order rate constant for the dissipation of response. A biological system should stay at steady state under normal condition when no drug intervention is applied. Therefore, at baseline $R_o = \frac{k_{in}}{k_{out}}$.

The four indirect response models under drug intervention are shown below:

$$\frac{dR}{dt} = k_{in}I(C_p) - k_{out}R \tag{1.72}$$

$$\frac{dR}{dt} = k_{in} - k_{out}I(C_p)R \tag{1.73}$$

$$\frac{dR}{dt} = k_{in}S(C_p) - k_{out}R \tag{1.74}$$

$$\frac{dR}{dt} = k_{in} - k_{out}S(C_p)R, \tag{1.75}$$

where $I(C_p) = 1 - \frac{C_p}{C_p + IC_{50}}$ represents the classical inhibitory function and $S(C_p) = 1 + \frac{E_{\max} \cdot C_p}{EC_{50} + C_p}$ is the stimulation process using an $E_{\max}$ model. The schematic representations of the indirect response models showing effect on the synthesis and dissipation processes are presented in Fig. 1.14.

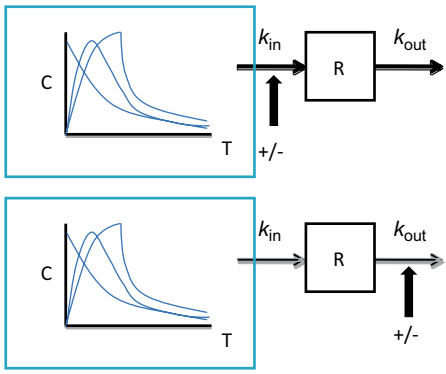

Fig. 1.14 Schematic representation of an indirect response—stimulation or inhibition of synthesis (*top*) and dissipation rates (*bottom*)

The indirect response model was used to fit to the data of the inhibition of prothrombin complex activity by warfarin, an oral anticoagulant used in thrombophlebities and pulmonary embolism (Jusko and Ko 1994). It blocks the vitamin K epoxide reductase, an enzyme that reduces vitamin K epoxide to vitamin K, which is a cofactor for carboxylation of the clotting factor such as factor II, VII, IX, and X. The blockade of the reductase activity by warfarin leads to the inhibition of coagulation, measured by the prothrombin time. It is assumed that the clotting factors are synthesized with a zero-order rate constant, k_{in}, and degraded with a first-order rate constant, k_{out}.

1.7 PD Models for Noncontinuous Response

Data collected from clinical trials, which are not continuous but categorical variables, can be dichotomous, ordinal scaled (e.g., none/mild/moderate/severe), or censored data (e.g., time to recurrence of a disease). Logistic regression and survival models are usually applied to describe the probability of events. Recently, Markov chain models to estimate event probability were also applied in pharmacometrics (Bizzotto et al. 2011; Lacroix et al. 2009; Sy et al. 2013a).

1.7.1 Time to Event

In the time to event analysis, the time of origin in pharmacometric analysis is usually the start of treatment. If the endpoint is some events, such as the occurrence of an adverse event, relapse of a disease, death, etc., the observations, which are the difference between the time of the specific event and the time from the origin, are referred to as time to event data or survival times. The distribution of time to event data is usually not normal and the data are often "censored." Right censoring refers to data that the specific event of interest has not yet occurred when the subjects

leave the study. Left censoring can occur in clinical studies when we know that the event of interest has already occurred at the observation time, but it is not known exactly when. For example, a patient may be tested positive for a specific disease but the exact time of the disease onset is unknown.

The survivor function, $S(t)$, is defined as the probability that the event of interest has not occurred by duration t, such that

$$S(t) = \Pr\{\mathrm{T} > t\} \tag{1.76}$$

where T denotes the time of an event; Pr stands for probability. The probability that the event has occurred by duration t, $F(t)$, is defined as the complement of the survivor function, which is 1-$S(t)$. The survivor function is related to the hazard function $h(t)$ and the cumulative hazard $H(t)$, as defined in Eqs. 1.77–1.79 (Collett 1994). One can obtain the hazard function by dividing the event density function $f(t)$ by the survivor function.

$$S(t) = \exp\left[-H(t)\right] \tag{1.77}$$

$$h(t) = \lim_{\Delta \to 0} \frac{\Pr\{t < T \le t + \Delta \mid T > t\}}{\Delta} = \frac{f(t)}{S(t)} = -\frac{\partial \log S(t)}{\partial t} \tag{1.78}$$

$$H(t) = -\log S(t). \tag{1.79}$$

Figure 1.15 shows representative examples of cumulative distribution, probability density, survival, and hazard functions.

With nonparametric and semi-parametric methods, namely the Kaplan–Meier estimate of the survivor function and the Cox proportional hazard model, which is an extension of the Kaplan–Meier method, the form of the baseline hazard is not specified. The form of the covariate relationship, however, is specified in the Cox proportional hazard model.

With parametric models, both the hazard function and the effect of covariates are explicitly defined. Holford argued for using a parametric model for the hazard function because "hazard is the way to introduce biological mechanism to the survival model and understanding the variability of time to event distributions" (Holford 2013). Table 1.4 lists the density, hazard, and survivor functions for the commonly used parametric models. Figure 1.15 shows the example of the probability density function and the corresponding hazard function for the exponential and Weibull distributions. In the exponential example, the hazard is a constant over time. This may not be the case in most clinical situations.

The Weibull model is more flexible as well as more generalized than the exponential model; the hazard rates are monotonic in the sense that the hazard is either increasing, decreasing, or constant over time. The hazard for a Weibull cannot be

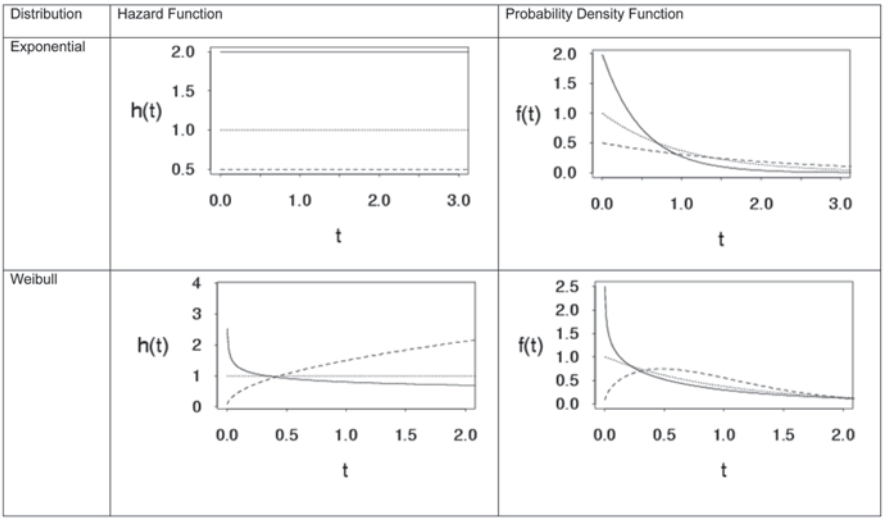

Fig. 1.15 Example of baseline hazard and the corresponding probability density functions for exponential and Weibull distribution

a combination of increasing and decreasing trends. The shape parameter, p, determines the trend. When $p<1$, the hazard is decreasing monotonically. For $p>1$, the hazard is increasing with time. With $p=1$, the Weibull becomes an exponential function and the hazard is constant. The log-logistic model allows for nonmonotonic hazards. The shape parameter, p, determines the trend such that if $p>1$, then the hazard increases and then declines whereas if $p<1$, the hazard has a decreasing trend.

The Kaplan–Meier type estimate is useful for determining the appropriate hazard function to use. The ratio of the number of events (δ_j) and the number of individuals at risk at the time ($n_j\tau_j$) is the hazard in the time interval from t_j to t_{j+1}:

$$h(t)=\frac{\delta_j}{n_j\tau_j}, \tag{1.80}$$

where n_j is the number of individual who has not had the event and therefore at risk of the event and τ_j is the time interval computed as $t_{j+1}-t_j$. The plot of time versus $h(t)$ provides a visual inspection of the trend of the hazard function.

The proportional hazard is one of the methodologies to introduce and evaluate a nontime-varying covariate effect, the other being accelerated failure time, which will not be discussed. Assuming a set of nontime-varying covariate vector $X=\left[X_1,X_2,\cdots,X_n\right]$, the proportional hazard function can be setup as

$$h(t,X)=h_0(t)\exp(\beta^T X), \tag{1.81}$$

Table 1.4 Relationship between density, survival, hazard, and likelihood functions for exponential, Weibull, and log-logistic parametric models

Parametric model	Density, f(t)	Survival,S(t)	Hazard, h(t)	Likelihood, L
Exponential	$\lambda \exp(-\lambda t)$	$\exp(-\lambda t)$	λ	$\prod_{i=1}^{N}\left\{\lambda \exp(-\lambda t)\right\}^{e_i}\left\{\exp(-\lambda t)\right\}^{1-\delta_i}$
Weibull	$\lambda p(\lambda t)^{p-1}\exp(-\lambda t)^{p}$	$\exp(-\lambda t)^{p}$	$\lambda p(\lambda t)^{p-1}$	$\prod_{i=1}^{N}\left\{\lambda p(\lambda t)^{p-1}\exp(-\lambda t)^{p}\right\}^{\delta_i}\left\{\exp(-\lambda t)^{p}\right\}^{1-\delta_i}$
Log-logistic	$\dfrac{\lambda^{p}t^{p-1}}{\left\{\frac{1}{p}\left[1+(\lambda t)^{p}\right]\right\}^{2}}$	$\dfrac{1}{1+(\lambda t)^{p}}$	$\dfrac{\lambda^{p}t^{p-1}}{\frac{1}{p}\left[1+(\lambda t)^{p}\right]}$	$\prod_{i=1}^{N}\left\{\dfrac{\lambda^{p}t^{p-1}}{\left\{\frac{1}{p}\left[1+(\lambda t)^{p}\right]\right\}^{2}}\times\dfrac{1}{1+(\lambda t)^{p}}\right\}^{\delta_i}\left\{\dfrac{1}{1+(\lambda t)^{p}}\right\}^{1-\delta_i}$

where $h_0(t)$ is the baseline hazard that depends on t but not X and $\beta^T X$ is $\beta_1 X_1 + \beta_2 X_2 + \cdots + \beta_n X_n$. A covariate, for example the presence of a specific disease, has an effect on the hazard and the coefficient, $\beta_{disease} = 1.39$. The relative risk for individuals with the disease is approximately fourfold (since $\exp(1.39) = 4$) that of the healthy individual. We recently applied the proportional hazard model in pharmacogenomics to evaluate the influence of *CYP3A5* and *ABCB1* polymorphisms on the renal transplant patient's relative risks for adverse events associated with tacrolimus (Sy et al. 2013b). The study used a marginal proportional hazard model with common baseline hazard to adjust for possible correlations between multiple incidents of adverse events, given that each patient can have multiple adverse events which were considered competing risks (Sy et al. 2013b; Wei et al. 1989; Wei and Glidden 1997). The marginal semi-parametric model is not without its criticism. The most frequent concern being raised is its assumption that each individual is considered to be at risk of all recurrent events from the start (Metcalfe and Thompson 2007). This assumption apparently would result in estimates that exceed those provided by alternative approaches. However, the marginal approach is considered to be the lesser of the two evils, with the alternative being one that does not consider a marginal model for repeated events from the same individual. For the parametric approach, the frailty model where the random effect has a multiplicative effect on the hazard can be used to handle recurrent events coming from the same individual. As pointed out by Hougaard, the limitation of the frailty model is the standard assumption of using a gamma distribution for frailty which puts more importance on late events (Hougaard 1995).

One can treat frailty as multiplicative of the hazard term such that

$$h(t_{ij} \mid \boldsymbol{X}_{ij}, \nu_i) = h_0(t_{ij})\nu_i \exp(\beta \boldsymbol{X}_{ij}), \tag{1.82}$$

where j refers the individual and i is the subgroup, and the frailty term is $\nu_i = \exp(W_j \psi)$. W_j is the "frailty" sampled from a distribution with mean 0 and a variance 1. If ψ is 0, we have a standard proportional hazard. The hazard rate above is conditional on both the covariates and the frailty term and so is the survivor function,

$$S\left(t_{ij} | \boldsymbol{X}_{ij}, \nu_i\right) = \exp\left(-\int_0^t h(u \mid \nu) du\right) = \exp\left(-\nu \int_0^t h(u)\, du\right). \tag{1.83}$$

Before we obtain the marginal survivor function, we shall introduce the gamma distribution. The density for the gamma distribution is given by

$$g(\nu, \alpha, \beta) = \frac{1}{\beta^{\alpha} \Gamma(\propto)} \nu^{\propto -1} e^{-\nu/\beta}, \tag{1.84}$$

where $\propto = \frac{1}{\theta}$, $\beta = \theta$, and the gamma integral is given by $\Gamma(\propto) = \int_0^{\infty} \nu^{\propto -1} e^{-\nu}$. By adopting the gamma distribution, $g(\nu)$, the expected survivor function can be derived:

$$S(t) = E\left[S\left(t_{ij} \mid \boldsymbol{X}_{ij}, \nu_i\right)\right] = E\left[\exp\left(-\int_0^t h(u \mid \nu) du\right)\right] = \mathrm{L}\left[\exp\left(\int_0^t h(u)\, du\right)\right], \quad (1.85)$$

where L is the Laplace transformation to integrate out the distribution of the frailty term.

Using the Weibull model as an example, the marginal Weibull survivor function with gamma frailty is such that

$$S(t) = \left[1 + \theta(\lambda t)^p\right]^{-1/\theta} \quad (1.86)$$

and the Weibull hazard with gamma frailty is equal to

$$h(t) = \lambda p(\lambda t)^{p-1}\left[S(t)\right]^{\theta}. \quad (1.87)$$

The frailty model is applicable in the clinical setting. For example, when a population is heterogeneous, it is likely that the population composition over time will consist of the more robust individuals as the frail ones failed. In such case, the overall population hazard is declining while individual hazards increase. The frailty term allows for the overall population hazard to decrease regardless of the individual hazard shape. The frailty model is more suited for the population approach in this respect.

For time-varying covariates, which are very applicable in the pharmacometric setting wherein the effect of drug concentration on the risk or hazard is a dynamic variable, the hazard should vary over time. Holford provided a tutorial explaining how the treatment effect can be incorporated to the hazard function to evaluate the dynamic drug time course on the hazard over time (Holford 2013).

1.7.2 Logistic Regression

A logistic regression is suitable for establishing relationship between the outcome of binary response data and explanatory variables (predictors). The probability of having an event is defined as:

$$\pi(x) = \frac{\exp(L(x))}{1 + \exp(L(x))} \quad (1.88)$$

where $\pi(x)$ is called logistic function with values between 0 and 1. $L(x)$ is a linear function of predictors, $L(x) = \beta_0 + \beta_1 x + \cdots + \beta_i x_i$, where β_0 is the intercept and $\beta_1, \ldots \beta_i$ are the coefficients, and x represents the predictors, such as drug concentration (Heiberger and Holland 2004; Venables et al. 1994).

We take the probability of no event, which is one subtract the previous probability, $\pi(x)$:

$$1-\pi(x)=\frac{1+\exp(L(x))-\exp(L(x))}{1+\exp(L(x))}=\frac{1}{1+\exp(L(x))}. \tag{1.89}$$

The odds describe the relative risk such that:

$$\frac{\pi(x)}{1-\pi(x)}=\frac{\exp(L(x))/\left[1+\exp(L(x))\right]}{1/\left[1+\exp(L(x))\right]}=\exp(L(x)). \tag{1.90}$$

Taking the natural logarithm of the odds above gives the $logit(L)$:

$$logit(L)=\log\left(\frac{\pi(x)}{1-\pi(x)}\right)=L(x). \tag{1.91}$$

The logit is no longer bounded and its value can take from $-\infty$ to $+\infty$. It is important to note that the error around the logit follows a binomial distribution rather than a normal distribution.

The generalized logistic regression model extends the analysis to multiple categorical response data or multinomial responses (Agresti 1999). The approach is to model cumulative logits by comparing each response category with baseline such that

$$\log\frac{\pi_i(\boldsymbol{x})}{\pi_{baseline}(\boldsymbol{x})}=\beta_{i0}+\boldsymbol{\beta}'_i\boldsymbol{x}, \tag{1.92}$$

where the subscript i represents the $i-1$ levels of response categories plus the baseline, $\pi_i(\boldsymbol{x})=P(Y=i|\boldsymbol{x})$ and $\sum_i\pi_i(\boldsymbol{x})=1$. This approach is often called the proportional odds assumption (McCullagh 1980; Peterson and Harrell 1990):

$$\text{logit}\left[P(Y\le i|\boldsymbol{x}\right]=\beta_{i0}+\boldsymbol{\beta}'\boldsymbol{x} \tag{1.93}$$

The comparison between two responses is then

$$\log\frac{\pi_a(\boldsymbol{x})}{\pi_b(\boldsymbol{x})}=\log\frac{\pi_a(\boldsymbol{x})}{\pi_{baseline}(\boldsymbol{x})}-\log\frac{\pi_b(\boldsymbol{x})}{\pi_{baseline}(\boldsymbol{x})}. \tag{1.94}$$

Sheiner in 1994 used the proportional odds model with individual specified random effects for the analysis of a 4-degree pain scale. The nonlinear mixed-effects model of ordered categorical PD data is mostly based on the proportional odds model and has been widely used for the evaluation of both efficacy and adverse events (Cullberg et al. 2005; Gomeni et al. 2001; Gupta et al. 1999; Johnston et al. 2003; Knibbe et al. 2002; Kowalski et al. 2003; Lunn et al. 2001; Mandema and Stanski 1996; Mould et al. 2001, 2002; Olofsen et al. 2005; Xie et al. 2002; Zingmark et al. 2003).

Kjellsson et al. presented a differential odds model to circumvent the assumption with the proportional odds model that the size of the predictor effect is the

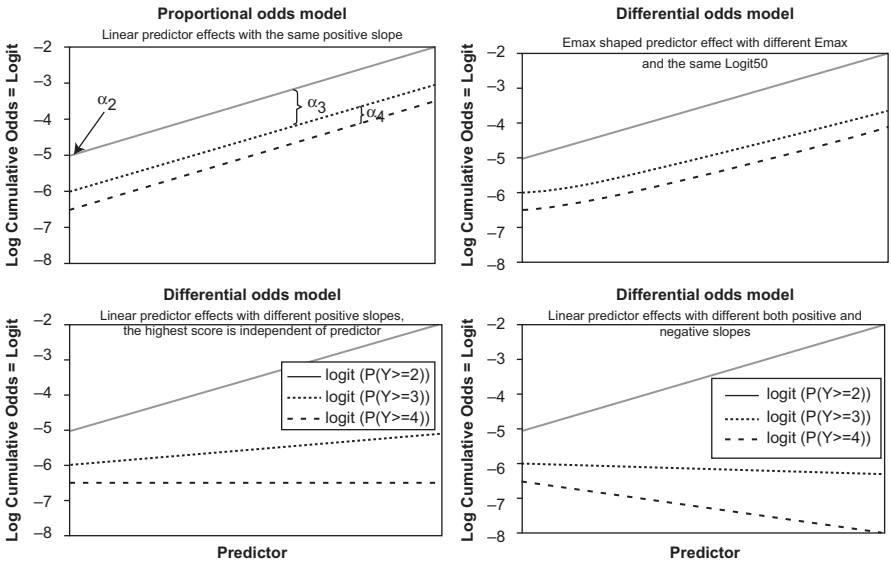

Fig. 1.16 Logit functions based on proportional odds versus differential odds models and their effects on the cumulative log odds. Examples include proportional odds model with linear predictor effects of the same slope (*upper left*), differential odds model using E_{max}-shaped predictor with variable E_{max} values (*upper right*), linear predictor with variable but positive slopes (*lower left*), and linear function with both positive and negative slopes (*lower right*). α_2 for baseline logit with score ≥ 2, α_3 and α_2 for baseline-shifted logit with score ≥ 3 and ≥ 4, respectively. (Image from Kjellsson et al. 2008, used with permission)

same for the log odds for all categories (Kjellsson et al. 2008). They argued that the assumption is valid for categories on a continuous scale but would not hold for categories based on ranking scale. Even though historically, the partial proportional odds model has been used to allow for variable sizes of predictor effect, some of the categories within the model have odds that are proportional to each other. While the predictor function is identical for the proportional odds model, the differential odds model allowed this function to vary. The model was implemented using cumulative probabilities so that the correct probability value can be allocated to a specific score or category (for example, mild score is more likely than severe score for a response such as sedation). Figure 1.16 illustrates the predictor versus log cumulative odds in proportional and differential odds model. In the upper left-hand corner, the slopes of the log cumulative odds versus the predictor graph are the same for the proportional odds model. The remaining graphs illustrate the log-cumulative odds versus predictor trend with differential odds model. The E_{max}-shaped predictor effects in the upper right all had positive slopes whereas mixtures of positive and negative slopes are possible with the alternative implementation.

1.7.3 Markov Chain

Another methodology in pharmacometrics that is gaining popularity for the analysis of categorical response variable is the Markov chain model, which has been applied in clinical studies. A Markov chain process is a probability model in which the distribution of future outcomes depends only on the current state and not on the whole history; this is often referred to as the memoryless property of a Markov chain (Bass 2011). In other words, the probability of a certain state to occur in the following time interval is only dependent on the state in the current time frame. With this definition, we suppose that a process in state i has a fixed probability P_{ij} that it will be in the next state j, such that

$$P\left\{X_{n+1} = j \middle| X_n = i\right\} = P_{ij}, \tag{1.95}$$

where the set $\left\{X_n, n = 0,1,2,\cdots\right\}$ is a stochastic process of finite possible outcomes and P_{ij} is often referred to as transition probability.

For this discussion, we shall use the example of early and late tacrolimus-related adverse event occurrence in stable pediatric renal allograft recipients after transplantation (Sy et al. 2013a). The transition probabilities were defined based on two states: without (state 0) and with (state 1) adverse event. A Markov chain model was chosen in that study because the observations may not be independent since it was assumed that the occurrence of an adverse event is related to the drug concentration. The current state of the patient was conditioned on his previous visit. The transition probabilities were: P_{00} for those who did not report an adverse event at a particular visit given no adverse event in the previous visit; P_{01} if the patient without adverse event in the previous visit reported an adverse event in the current visit; P_{10} for patients with an adverse event in the previous visit but no adverse event in the current one; and P_{11} if an adverse event occurred on both visits. The transition probabilities adhered to Markov properties such that the sum of the transition probabilities from the specific state is 1:

$$\sum_{j=0}^{1} P_{ij} = 1. \tag{1.96}$$

The function that is utilized for the estimation of the transition probabilities varies depending on the study needs. Kemp and Kamphuisen simulated human hypnograms using a Markov chain model (Kemp and Kamphuisen 1986). Karlsson et al. parameterized the transition probabilities through binary logistic function to describe sleep data (Karlsson et al. 2000). Bizzotto et al. utilized a multinomial logistic function to characterize the time course of transition probabilities between sleep stages in insomniac patients (Bizzotto et al. 2010, 2011). Ouellet et al. used a logistic regression wherein the logit function is linear to estimate the transition probability of having an adverse event due to dizziness in subjects who were administered a selective glycine transporter 1 inhibitor (Ouellet et al. 2011). An example in Ross

probability textbook adopted Poisson probability density function (pdf) for counting process in the estimation of transition probability (Ross 2006). The Poisson pdf assumes that the magnitude of the variance is identical to its mean. However, many counting processes show greater variability than that predicted by the Poisson model. Troconiz et al. explored mixed Markov elements and Poisson distribution to evaluate overdispersion in the variance of a Poisson distribution (Troconiz et al. 2009). There are numerous other implementations of the transition probability which we cannot possibly list all of them in this introductory chapter. When selecting whether or not to use a Markov model, Karlsson suggested that the Markov model is more suitable for consecutive same-state observations, which are typical for sleep patterns, as an example (Karlsson et al. 2000).

1.8 Disease Progression Model

The natural time course of a disease is often not one that is static but becomes progressively worse if left untreated. The disease trajectory is not constant, unlike the common assumption that is taken when using the E_{max} model wherein the baseline E_0 is static. Even as early as the 1970s, investigators reported longitudinal studies of the natural history of non-Hodgkin's lymphoma stages and coronary artery stenosis (Fuller et al. 1975; Rosch et al. 1976). A disease progression model describes how an indicator for the disease or a clinically relevant endpoint changes in time. For the purpose of modeling disease progression, the approach has been applied in degenerative diseases such as Alzheimer's disease (Holford and Peace 1992a, b), schizophrenia (Kimko et al. 2000), and diabetic neuropathy (Bakris et al. 1996; Bjorck et al. 1992; Crepaldi et al. 1998; Gall et al. 1993; Lewis et al. 1993; Parving et al. 1995).

Most of the disease progression models are empirical that describe the disease trajectory rather than its physiological background. The linear model has the following general form of equation that characterizes the disease as changing linearly with time:

$$S(t) = S_0 + \alpha t, \tag{1.97}$$

where $S(t)$ represents the disease status at a specific time t, S_0 is the baseline that can be constant or a time-dependent function (e.g., sinusoidal function to characterize circadian rhythm), and $\propto$ is the slope of the linear process. Therapeutic interventions, including placebo, can change the trajectory of a disease process. Interventions are generally classified as either symptomatic or disease modifying. Let $f(T)$ be the function to characterize the effect of treatment or intervention. In the case of symptomatic treatment, the effect of intervention would shift the disease baseline but not change the slope whereas disease-modifying interventions would change the rate of disease progression, as shown in Eqs. 1.98 and 1.99, respectively (Mould 2007; Mould et al. 2007; Schmidt et al. 2011):

$$S(t) = S_0 + f(T) + \alpha t \tag{1.98}$$

$$S(t) = S_0 + (f(T) + \alpha)t \tag{1.99}$$

From the two equations above, the symptomatic interventions have different effect on the disease status from disease-modifying interventions. The disease trajectory will revert to its natural progression rate α once the treatment is discontinued, regardless of the type of treatment. A third type of intervention is one that exerts completely cure and reverses the disease status back to pre-disease state. This type of intervention may best be characterized by a model that incorporates both symptomatic and disease-modifying effect:

$$S(t) = S_0 + f_1(T) + (f_2(T) + \alpha)t \tag{1.100}$$

In the examples listed previously of applications of disease progression modeling approach in specific therapeutic areas, the linear disease progression was used by Kimko et al. to study the effect of quetiapine fumarate, an antischizophrenic agent, on schizophrenia status based on the Brief Psychiatric Rating Scale (Kimko et al. 2000).

Nonlinear functions have also been used as disease progression model. Pors-Nielsen and Friberg used an exponential model to describe the effect of estrogen/progestin treatment on osteoporosis (Pors Nielsen et al. 1994). Grantham et al. also used a similar model to describe the increase in renal volume in autosomal dominant polycystic kidney disease (Grantham et al. 2008). Pillai et al. utilized an indirect response type model to investigate biomarker response to ibandronate (Pillai et al. 2004).

1.9 Systems Pharmacology

Molecular biology evaluates single genes and proteins while systems biology combines the complex interactions at all levels of a biological system. By viewing all levels of biological information in the process, scientists are able to determine important properties of the system. Mathematical models of biological processes help describe time-dependent kinetic behavior and causality. The mechanistic approach to modeling systems' biological processes is based on sound biological principles with prior knowledge about the biochemical network involved. The variables and parameters are related to a physiological or cellular process where the information is obtained from an *in vitro* or physiological experiment. This approach gives the scientist a holistic view of the biological system. The study of mechanism of drug action on the system itself also becomes more precise.

One of the systems level models applied in drug development is that of the regulation of glucose. Landersdorfer and Jusko provided an excellent review of application of modeling in diabetes, with a specific focus on modeling drug effects (Land-

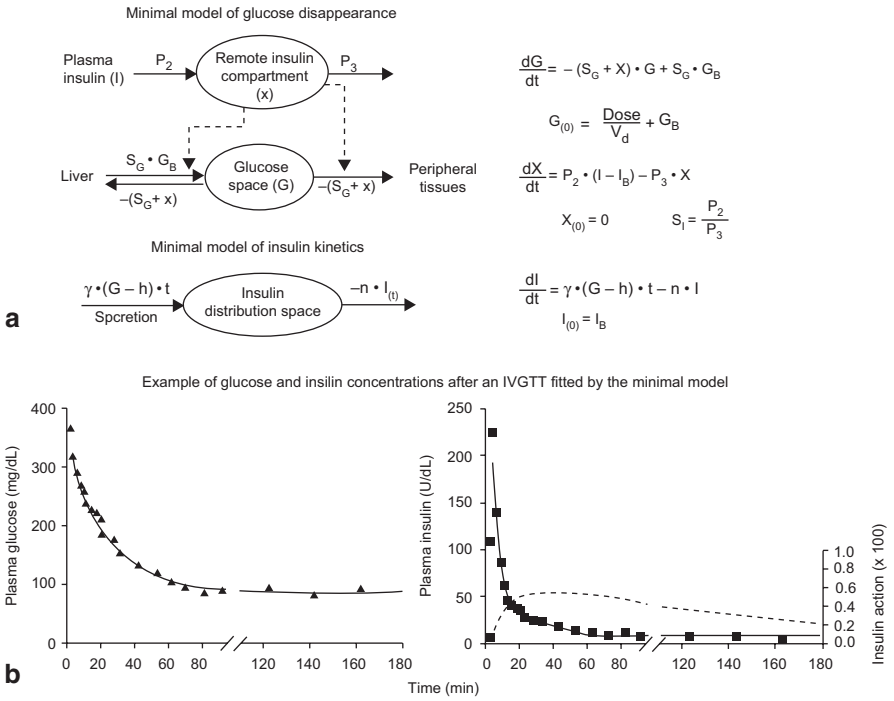

Fig. 1.17 Structure and equations of the minimal model of insulin-glucose feedback and control (*top*) and example of glucose and insulin concentrations after an IV glucose tolerance test fitted by the minimal model. (Image from Landersdorfer and Jusko 2008, used with permission)

ersdorfer and Jusko 2008). In 1979, Bergman et al. developed a minimal model that included three coupled differential equations to describe the intravenous glucose tolerance test (Bergman et al. 1979). Using several feedback control mechanisms, the model couples insulin I and glucose G regulation and also introduces an additional unobserved insulin component X to describe the delay between insulin release and the response characterized by the reduction in blood glucose (Fig. 1.17):

$$\begin{aligned}\frac{dG}{dt} &= -(S_G + X(t)) \cdot G(t) + S_G \cdot G_B \\ \frac{dX}{dt} &= p_2 \cdot (I(t) - I_B) - p_3 \cdot X(t) \\ \frac{dI}{dt} &= \gamma \cdot (G(t) - h)t - n \cdot I(t)\end{aligned} \tag{1.101}$$

The baseline values were h, G_B and I_B and parameters were S_G, p_2, p_3, γ, and n. The initial conditions were such that

$$G(0) = \frac{Dose}{V_d} + G_B$$
$$X(0) = 0$$
$$I(0) = I_B \tag{1.102}$$

Though this model is widely used, it is not without its problems. The model does not allow both insulin and glucose to be fitted simultaneously (Pacini and Bergman 1986). The additional unobserved insulin effect compartment X is unbounded and can increase indefinitely when both glucose and insulin parts of the model were estimated simultaneously (De Gaetano and Arino 2000). Another issue with the model is that it does not take into account the first and second insulin phases (Agerso and Vicini 2003). This model is applicable for diagnostic test but limited for drug evaluation.

In the study of glucagon-like peptide-1 analog NN221, Agerso and Vicini introduced a Gaussian term to describe the first-phase insulin secretion (Agerso and Vicini 2003). The resulting equation for I was such that

$$\frac{dI}{dt} = \beta(t) + \gamma \cdot (G(t) - h)t - n \cdot I(t), \tag{1.103}$$

where $\beta(t)$ is an empirical Gaussian function that accounts for the amplitude of the first-phase insulin as well as duration of this process. Mager et al. (2004) further modified the γ parameter to an $E_{\max}$ model to include a drug effect for another GLP-1 analog, exenatide (Mager et al. 2004). This model was used in the analysis of data from hyperglycemic clamp study in healthy subjects and diabetic patients.

Indirect response type models have been applied to study the effects of various antidiabetic agents on glucose and insulin. Benincosa and Jusko evaluated rosiglitazone effects wherein both fasting plasma glucose (FPG) and hemoglobin A1c (HbA1c) were measured (Benincosa and Jusko 1999). The glycosylation of hemoglobin was described by a second-order process that is proportional to the FPG concentrations and is dependent on the ratio of the steady-state HbA1c and FPG. The elimination of HbA1c is a first-order process. Hamren et al. modified the model for tesaglitazar such that the glycosylation process also takes into account the erythrocyte lifespan and utilizes several transit compartments to describe the aging process of erythrocytes (Hamren et al. 2008).

Given that diabetes is a chronic disease that becomes progressively worse, the models should also examine disease progression for long-term studies of antidiabetic drugs. Frey et al. investigated the effect of sustained-release gliclazide on FPG over 10 weeks to 1 year period (Frey et al. 2003). In patients who responded to the treatment, FPG levels initially declined and then slowly increased whereas the nonresponders' FPG levels continued to increase in the natural disease progression process. The authors utilized an empirical linear model with an intercept and a positive slope to describe the disease progression, measured by FPG over time:

$$FPG(t) = baseline + \alpha \cdot t - E_t, \tag{1.104}$$

where α is the slope of the disease progression process, E_t is the predicted treatment effect at the time when the treatment was administered, and baseline is the predicted baseline FPG. Since gliclazide was assumed to only alleviate the symptoms of the disease without modifying the disease itself, the effect of the drug was to shift the curve without affecting the rate of disease progression that is characterized by the α term.

De Winter et al. modeled the worsening of β cell activity (B) and insulin sensitivity (S) using a different disease progression model approach (de Winter et al. 2006):

$$\begin{aligned} B &= \frac{1}{1+\exp(b_0 + r_b \cdot t)} \\ S &= \frac{1}{1+\exp(s_0 + r_s \cdot t)} \end{aligned} \tag{1.105}$$

where baselines were b_0 and s_0 and rates of disease progression were r_b and r_s. Their investigation also included a model for HbA1c, which was fitted simultaneously along with FPG and insulin levels.

More sophisticated models of the whole body have been developed and focused on tissues and organs that are relevant in diabetes. These models were used to simulate virtual patients and predict clinical trial outcomes. As these complex models are relatively difficult to develop, many assumptions are made and model parameters are often taken from literature. Examples of these models include the Archimedes, the Entelos Metabolism, and T1Dm PhysioLab®. As these models are proprietary, there is a lack of transparency in the model equations and parameter values (Herman 2003).

Another therapeutic area where systems biology and pharmacology models are extensively used is in oncology. Biochemical reactions and signaling pathways are often described by differential equations that characterize a chemical reaction. Most of these processes involve a complex network of chemical and biochemical reactions. The *law of mass action* is the common convention that is used to describe the rate at which chemical entities interact to form a different combination. The computational model for heregulin-induced p-ErBB3 signaling and the effect of antibody inhibitors pertuzumab and lapatinib utilizes such convention (McDonagh et al. 2012; Schoeberl et al. 2009). The following chemical reactions were listed for ErbB2/3-bispecific antibody binding and receptor cross-linking:

$$E2 + BsAb \leftrightarrow E2 : BsAb \tag{1.106}$$

$$BsAb + E3 \leftrightarrow BsAb : E3 \tag{1.107}$$

$$E2 + BsAb : E3 \leftrightarrow E2 : BsAb : E3 \tag{1.108}$$

$$E2:BsAb+E3\leftrightarrow E2:BsAb:E3 \tag{1.109}$$

where E2 and E3 represent ErbB2/3, respectively, and BsAb refers to a bi-specific antibody. The chemical reactions listed in Eqs. 1.106–1.109 are reversible processes and the reaction schema can be generalized:

$$A+B\xrightarrow{k}C\xrightarrow{k'}A+B \tag{1.110}$$

where k is the forward reaction rate and k' is the reversible rate. The rate of change for each of the above species can be written as follows:

$$\begin{aligned}\frac{d[A]}{dt}&=k'[C]-k[A][B]\\ \frac{d[B]}{dt}&=k'[C]-k[A][B]\\ \frac{d[C]}{dt}&=k[A][B]-k'[C]\end{aligned} \tag{1.111}$$

As one can see, writing out the differential equations for the chemical reaction in Eq. 1.111 becomes a tedious effort, especially when the biological system has many players. Some systems biology tools allow user to create reaction processes and will automatically create the corresponding differential equations in the background (Maiwald and Timmer 2008).

In identifying targets, McDonagh et al. utilized computation modeling and cell signaling insights to develop specific targeted antibodies that are capable to destabilize the over expression of ErbB2 by inhibiting ErbB3 signaling (McDonagh et al. 2012). They identified that ErbB3/heregulin activation plays a critical role in ErbB2-positive refractory disease and that the synergy can be achieved in combination therapies involving ErbB3 inhibitor and ErbB2 therapies (McDonagh et al. 2012). System pharmacology models are slowly being adopted in drug development settings and the examples show promising prospect for systems pharmacology to become part of mainstream pharmacometric analyses.

1.10 Software

As software facilitates PKPD modeling and simulation, we will discuss the available software packages that have been used for different types of analyses. For noncompartmental analysis (or statistical moment approach), WinNonlin is most commonly used in the pharmaceutical industry. Alternately, the PK package in R is a basic PK package that performs noncompartmental analysis of PK data as well. A brief description of this tool can be found on the CRAN project website (http://cran.r-project.org/web/views/Pharmacokinetics.html). For nonlinear mixed effect modeling, NONMEM is the most commonly used software in the drug development

setting. The Non-Parametric Adaptive Grid algorithm using NPAG (USC*PACK) is common for modeling population PK data in the therapeutic drug monitoring setting. The other software for mixed effect modeling are ADAPT that is based on important sampling algorithm, MONOLIX with the Markov Chain Monte Carlo (MCMC) stochastic approximation expectation maximization (SAEM). BUGS is a software package for performing Bayesian inference using Gibbs sampling. The user specifies a statistical model by stating the relationships between related variables. The software determines an appropriate MCMC scheme (based on the Gibbs sampler) for analyzing the specified model. The user then controls the execution of the scheme. There are two main versions of BUGS, namely WinBUGS and OpenBUGS. The recent release of NONMEM has incorporated the algorithms in the other software packages mentioned above. SimCyp includes a population-based simulation system using PBPK model.

For systems biology modeling, the Matlab platform and specialized toolboxes that were built on top of the Matlab platform can handle large and complex models that may contain hundreds of coupled differential equations. The large models can be slow in Matlab. Specialized Matlab toolbox such as Potterswheel (URL: potterswheel.de) utilizes chemical reaction scheme and builds the corresponding differential equations in C language to speed up the analysis and fitting processes (Maiwald and Timmer 2008). Curated systems biology models are available from library consortiums that are publicly accessible (e.g., http://www.ebi.ac.uk/biomodels-main) and can be ported to specialized software packages through Systems Biology Markup Language (SBML).

1.11 Conclusion

Over the past decade, pharmacometrics has become a discipline that is frequently utilized in academia, worldwide regulatory agencies, and the biopharmaceutical industry. Cost cutting and improvement in drug development will come from creative application of pharmacometric modeling approach.

The US FDA has emphasized the importance of model-based drug development wherein PK/PD models to characterize drug efficacy and safety are being developed for both preclinical and clinical data. The agency strongly supports this program, “Pharmacometric analyses, we believe, are valuable to gain insights into the data across drugs and to plan future development. The model and simulation approaches should not be viewed as substitutes to conducting clinical trials in all instances. Also, such quantitative analyses should not be primarily used to ‘rescue’ failed trials for seeking approval. Where appropriate, the FDA accepted simulation results” (Bhattaram et al. 2005).

Appendix

Derivation of Eq. 1.55

Implicit in the assumption that the concentration of drug in the system that is being cleared is constant or at steady state, we assumed that the rate of change in the drug concentration is 0 and thus set all the left-hand sides in the list of equations in Eq. 1.53 to 0.

$$0 = V_1 \frac{dC_{1(vein)}}{dt} = Q_1 \cdot C_0 - Q_1 \cdot C_1 + K_I(t) \tag{1.112}$$

$$0 = V_2 \frac{dC_{2(artery)}}{dt} = Q_1 \cdot C_{3o} - Q_1 \cdot C_2 \tag{1.113}$$

$$0 = V_3 \frac{dC_{3(lung)}}{dt} = Q_1 \cdot C_1 - Q_1 \cdot C_{3o} - r_3(C_3) \tag{1.114}$$

$$0 = V_4 \frac{dC_{4(liver)}}{dt} = Q_7 \cdot C_{7o} + (Q_4 - Q_7) \cdot C_2 - Q_4 \cdot C_{4o} - r_4(C_4) \tag{1.115}$$

$$0 = V_5 \frac{dC_{5(kidney)}}{dt} = Q_5 \cdot C_2 - Q_5 \cdot C_{5o} - r_5(C_5) \tag{1.116}$$

$$0 = V_6 \frac{dC_{6(rest\ of\ body)}}{dt} = Q_6 \cdot C_2 - Q_6 \cdot C_{6o} \tag{1.117}$$

$$0 = V_7 \frac{dC_{7(GI\ tract)}}{dt} = Q_7 \cdot C_2 - Q_7 \cdot C_{7o} - r_7(C_7). \tag{1.118}$$

From Eq. 1.112, we integrate

$$\int_0^\infty Q_1 \cdot C_1 \, dt = \int_0^\infty (Q_1 \cdot C_0 + K_I(t)) dt. \tag{1.119}$$

By applying Eq. 1.54 and substituting $Q_1 \cdot C_0$ with $Q_4 \cdot C_{4o} + Q_5 \cdot C_{5o} + Q_6 \cdot C_{6o}$ to Eq. 1.119, the resulting expression is

$$Q_1 \int_0^\infty C_1 \, dt = \int_0^\infty (Q_4 \cdot C_{4o} + Q_5 \cdot C_{5o} + Q_6 \cdot C_{6o}) dt + \int_0^\infty K_I(\mathrm{t}) dt. \tag{1.120}$$

Rearrangement of Eq. 1.120 by adding and subtracting $(Q_7 \cdot C_{7o} + (Q_4 - Q_7) C_2 + Q_5 \cdot C_{5o} + Q_6 \cdot C_2)$ to Eq. 1.120 such that the net result is 0 will yield the following expression:

$$\begin{aligned} Q_1 \int_0^\infty C_1\, dt = \int_0^\infty & \left[(Q_7 \cdot C_{7o} + (Q_4 - Q_7) C_2 + Q_5 \cdot C_{5o} + Q_6 \cdot C_2) \right. \\ & \left. - (Q_7 \cdot C_{7o} + (Q_4 - Q_7) C_2 + Q_5 \cdot C_{5o} + Q_6 \cdot C_2) \right] dt \\ & + \int_0^\infty (Q_4 \cdot C_{4o} + Q_5 \cdot C_{5o} + Q_6 \cdot C_{6o}) dt + \int_0^\infty K_I(t) dt. \end{aligned} \quad (1.121)$$

From Eq. 1.117, $\int_0^\infty (Q_6 \cdot C_2 - Q_6 \cdot C_{6o}) dt = 0$. Given that $Q_7 \cdot C_{7o} + (Q_4 - Q_7) C_2$ represents the total amount of drug entering the liver from the artery and the gut which is also C_p, wherein $Q_4 \cdot C_p = Q_7 \cdot C_{7o} + (Q_4 - Q_7) C_2$, we can then simplify Eq. 1.121 as follows:

$$\begin{aligned} Q_1 \int_0^\infty C_1\, dt = & \int_0^\infty (Q_4 + Q_5 + Q_6) C_2 dt \\ & - \left\{ \int_0^\infty Q_4 (C_p - C_{4o}) dt + \int_0^\infty Q_5 (C_2 - C_{5o}) dt + \int_0^\infty Q_7 (C_2 - C_{7o}) dt \right\} \\ & + \int_0^\infty K_I(t) dt. \end{aligned} \quad (1.122)$$

Furthermore, $\int_0^\infty (Q_4 + Q_5 + Q_6) C_2 dt = Q_1 \int_0^\infty C_2 dt$, since $Q_1 = Q_4 + Q_5 + Q_6$ and from Eq. 1.113, $Q_1 \int_0^\infty C_{3o} dt$, then Eq. 1.122 can be rewritten as Eq. 1.55:

$$\begin{aligned} & \int_0^\infty Q_1 (C_1 - C_{3o}) dt + \int_0^\infty Q_4 (C_p - C_{4o}) dt + \int_0^\infty Q_5 (C_2 - C_{5o}) dt \\ & \qquad + \int_0^\infty Q_7 (C_2 - C_{7o}) dt = \int_0^\infty K_I(t) dt. \end{aligned}$$

Derivation of Eq. 1.60

Using the expression for mean clearance, the rearrangement of Eqs. 1.55 through 1.59 will result in the following:

$$\overline{CL}_{systemic} = \overline{CL}_3 + \left(\frac{\int_0^\infty C_p\, dt}{\int_0^\infty C_1\, dt} \right) \overline{CL}_4 + \left(\frac{\int_0^\infty C_2\, dt}{\int_0^\infty C_1\, dt} \right) (\overline{CL}_5 + \overline{CL}_7). \quad (1.123)$$

We set $Q_4 \cdot C_p = Q_7 C_{7o} + (Q_4 - Q_7) C_2$ to $Q_4 (C_2 - C_p) = Q_7 (C_2 - C_{7o})$. Then integrate the latter expression from 0 to infinity, $Q_4 \int_0^\infty (C_2 - C_p) dt = Q_7 \int_0^\infty (C_2 - C_{7o}) dt$ and divide both sides of the equation by $\int_0^\infty C_2 dt$ to obtain

$\frac{Q_4\int_0^\infty (C_2 - C_p)dt}{\int_0^\infty C_2 dt} = \frac{Q_7\int_0^\infty (C_2 - C_{7o})dt}{\int_0^\infty C_2 dt}$. The previous equation can be rewritten as

$1 - \frac{\int_0^\infty C_p dt}{\int_0^\infty C_2 dt} = \frac{Q_7\int_0^\infty (C_2 - C_{7o})dt}{Q_4\int_0^\infty C_2 dt}$. The ratio consisting the integrating components on the left side of the equation is the expression for the extraction ratio for tissue compartment 7 for the GI tract, $\bar{E}_7 = \frac{\int_0^\infty (C_2 - C_{7o})\mathrm{d}t}{\int_0^\infty C_2 \mathrm{d}t}$. Therefore,

$$\frac{\int_0^\infty C_p dt}{\int_0^\infty C_2 dt} = 1 - \frac{Q_7}{Q_4}\bar{E}_7 \tag{1.124}$$

From Eq. 1.113 above, $Q_1\int_0^\infty C_2 dt = Q_1\int_0^\infty C_3 dt$, and from Eq. 1.57, $\overline{CL}_3 = \frac{Q_1\int_0^\infty (C_1 - C_{3o})dt}{\int_0^\infty C_1 dt} = \frac{Q_1\int_0^\infty (C_1 - C_2)dt}{\int_0^\infty C_1 dt}$. Thus,

$$\frac{\int_0^\infty C_2 dt}{\int_0^\infty C_1 dt} = 1 - \frac{\overline{CL}_3}{Q_1} = 1 - \bar{E}_{lung} \tag{1.125}$$

In the following step, multiply Eq. 1.124 by A125:

$$\frac{\int_0^\infty C_p dt}{\int_0^\infty C_1 dt} = \left(1 - \frac{\overline{CL}_3}{Q_1}\right)\left(1 - \frac{\overline{CL}_7}{Q_4}\right). \tag{1.126}$$

Since $\overline{CL}_7 = Q_7 \cdot \bar{E}_7$. In the following step, we substitute Eqs. 1.126 and 1.125 to Eq. 1.123, $\overline{CL}_{systemic} = \overline{CL}_3 + \left(1 - \frac{\overline{CL}_3}{Q_1}\right)\left(1 - \frac{\overline{CL}_7}{Q_4}\right)\overline{CL}_4 + \left(1 - \frac{\overline{CL}_3}{Q_1}\right)(\overline{CL}_5 + \overline{CL}_7)$

$$= \overline{CL}_3 + (1 - \bar{E}_3)\left[\overline{CL}_4 + (1 - \bar{E}_4)\overline{CL}_7 + \overline{CL}_5\right].$$

References

Agerso H, Vicini P (2003) Pharmacodynamics of NN2211, a novel long acting GLP-1 derivative. Eur J Pharm Sci 19(2–3):141–150

Agoram B, Heatherington AC, Gastonguay MR (2006) Development and evaluation of a population pharmacokinetic-pharmacodynamic model of darbepoetin alfa in patients with nonmyeloid malignancies undergoing multicycle chemotherapy. AAPS J 8(3):E552–E563

Agresti A (1999) Modelling ordered categorical data: recent advances and future challenges. Stat Med 18(17–18):2191–2207

Andersen ME, Gargas ML, Ramsey JC (1984) Inhalation pharmacokinetics: evaluating systemic extraction, total in vivo metabolism, and the time course of enzyme induction for inhaled styrene in rats based on arterial blood:inhaled air concentration ratios. Toxicol Appl Pharmacol 73(1):176–187

Andersen ME, Clewell HJ 3rd, Gargas ML, Smith FA, Reitz RH (1987) Physiologically based pharmacokinetics and the risk assessment process for methylene chloride. Toxicol Appl Pharmacol 87(2):185–205

Bakris GL, Copley JB, Vicknair N, Sadler R, Leurgans S (1996) Calcium channel blockers versus other antihypertensive therapies on progression of NIDDM associated nephropathy. Kidney Int 50(5):1641–1650

Bass RF (2011) Stochastic processes, edn. Cambridge University Press, Cambridge

Baxter LT, Zhu H, Mackensen DG, Jain RK (1994) Physiologically based pharmacokinetic model for specific and nonspecific monoclonal antibodies and fragments in normal tissues and human tumor xenografts in nude mice. Cancer Res 54(6):1517–1528

Bellman RE, Jacquez JA, Kalaba RE, Kotkin B (1963) A mathematical model of drug distribution in the body: implications for cancer chemotherapy. Rand Corporation, Santa Monica, California.

Benet LZ (2010) Clearance (nee Rowland) concepts: a downdate and an update. J Pharmacokinet Pharmacodyn 37(6):529–539

Benet LZ, Galeazzi RL (1979) Noncompartmental determination of the steady-state volume of distribution. J Pharm Sci 68(8):1071–1074

Benincosa L, Jusko W (1999) Novel method of treatment. World Intellectual Property Organization, Geneva, Publ. no. W0/2000/027341

Bergman RN, Ider YZ, Bowden CR, Cobelli C (1979) Quantitative estimation of insulin sensitivity. Am J Physiol 236(6):E667–E677

Bernards JK (1986) A pharmacokinetic model for lung uptake of volatile chemicals. MChE, University of Delaware, Newark, DE (Master's thesis, advisor: K. Bischoff)

Bhattaram VA, Booth BP, Ramchandani RP, Beasley BN, Wang Y, Tandon V et al (2005) Impact of pharmacometrics on drug approval and labeling decisions: a survey of 42 new drug applications. AAPS J 7(3):E503–512

Bischoff KB (1966) Drug distribution in mammals. Chem Eng Med Biol 62(66): 33–45

Bischoff KB (1975) Some fundamental considerations of the applications of pharmacokinetics to cancer chemotherapy. Cancer Chemother Rep Part 1 59(4):777–793

Bischoff KB (1987) Physiologically based pharmacokinetic modeling, edn, Drinking Water and Health, Volume 8: Pharmacokinetics in Risk Assessment. National Academy Press, Washington, DC.

Bischoff KB (1992) PBPK models: what are we really assuming? Presentation at the Chemical Industry Institute of Toxicology Founders Award

Bischoff KB, Dedrick RL (1968) Thiopental pharmacokinetics. J Pharm Sci 57(8):1346–1351

Bischoff KB, Dedrick RL, Zaharko DS (1970) Preliminary model for methotrexate pharmacokinetics. J Pharm Sci 59(2):149–154

Bizzotto R, Zamuner S, De Nicolao G, Karlsson MO, Gomeni R (2010) Multinomial logistic estimation of Markov-chain models for modeling sleep architecture in primary insomnia patients. J Pharmacokinet Pharmacodyn 37(2):137–155

Bizzotto R, Zamuner S, Mezzalana E, De Nicolao G, Gomeni R, Hooker AC et al (2011) Multinomial logistic functions in markov chain models of sleep architecture: internal and external validation and covariate analysis. AAPS J 13(3):445–463

Bjorck S, Mulec H, Johnsen SA, Norden G, Aurell M (1992) Renal protective effect of enalapril in diabetic nephropathy. BMJ 304(6823):339–343

Boxenbaum H (1982) Interspecies scaling, allometry, physiological time, and the ground plan of pharmacokinetics. J Pharmacokinet Biopharm 10(2):201–227

Boxenbaum H, Ronfeld R (1983) Interspecies pharmacokinetic scaling and the Dedrick plots. Am J Physiol 245(6):R768–R775

Brandfonbrener M, Landowne M, Shock NW (1955) Changes in cardiac output with age. Circulation 12(4):557–566

Brindley PG, Dunn WF (2009) Simulation for clinical research trials: a theoretical outline. J Crit Care 24(2):164–167

Brown R, Delp M, Lindstedt S, Rhomberg L, Beliles R (1997) Physiological parameter values for physiologically based pharmacokinetic models. Toxicol Ind Health 13407:484

Burnham KP, Anderson DR (2002) Model selection and multi-model inference: a practical information-theoretic approach, Second edn. Springer

Chen HS, Gross JF (1979) Physiologically based pharmacokinetic models for anticancer drugs. Cancer Chemother Pharmacol 2(2):85–94

Collett D (1994) Modelling survival data in medical research, 1st edn. Chapman & Hall, New York

Collins JM, Dedrick RL (1983) Distributed model for drug delivery to CSF and brain tissue. Am J Physiol 245(3):R303–R310

Coxson PG, Bischoff KB (1987a) Lumping strategy. 1. Introductory techniques and applications of cluster analysis. Ind Eng Chem Res 26(6):1239–1248

Coxson PG, Bischoff KB (1987b) Lumping strategy. 2. System theoretic approach. Ind Eng Chem Res 26(10):2151–2157

Crepaldi G, Carta Q, Deferrari G, Mangili R, Navalesi R, Santeusanio F et al (1998) Effects of lisinopril and nifedipine on the progression to overt albuminuria in IDDM patients with incipient nephropathy and normal blood pressure. The Italian Microalbuminuria Study Group in IDDM. Diabetes Care 21(1):104–110

Cullberg M, Eriksson UG, Wahlander K, Eriksson H, Schulman S, Karlsson MO (2005) Pharmacokinetics of ximelagatran and relationship to clinical response in acute deep vein thrombosis. Clin Pharmacol Ther 77(4):279–290

Dayneka NL, Garg V, Jusko WJ (1993) Comparison of four basic models of indirect pharmacodynamic responses. J Pharmacokinet Biopharma 21(4):457–478

De Gaetano A, Arino O (2000) Mathematical modelling of the intravenous glucose tolerance test. J Math Biol 40(2):136–168

de Winter W, DeJongh, Moules I et al (2006) A mechanism-based disease progression model for comparison of long-term effects of pioglitazone, metformin and gliclazide on disease processes underlying Type 2 Diabetes Mellitus. J Pharmacokinet Pharmacodyn 33(3):313–343

Dedrick RL (1973) Animal scale-up. J Pharmacokinet Biopharma 1(5):435–461

Dedrick RL, Bischoff KB (1980) Species similarities in pharmacokinetics. Fed Proc 39(1):54–59

Derendorf H, Hochhaus G (1995) Handbook of pharmacokinetics/pharmacodynamics correlation, CRC Press, Boca Raton, FL

Derendorf H, Lesko LJ, Chaikin P, Colburn WA, Lee P, Miller R et al (2000) Pharmacokinetic/pharmacodynamic modeling in drug research and development. J Clin Pharmacol 40(12 Pt 2):1399–1418

DiSanto AR, Wagner JG (1972) Pharmacokinetics of highly ionized drugs. 3. Methylene blue–blood levels in the dog and tissue levels in the rat following intravenous administration. J Pharm Sci 61(7):1090–1094

Dunne A (1993) Statistical moments in pharmacokinetics: models and assumptions. J Pharm Pharmacol 45(10):871–875

European agency for the evaluation of medicinal products (2007) Guideline on reporting the results of population pharmacokinetic analyses. CHMP/EWP/185990/06 (available at http://www.ema.europa.eu/docs/en_GB/document_library/Scientific_guideline/2009/09/WC500003067.pdf)

Ette EI, Sun H, Ludden TM (1998) Balanced designs in longitudinal population pharmacokinetic studies. J Clin Pharmacol 38(5):417–423
Frank GT (1982) A physiological pharmacokinetic model of the lung. MChE, University of Delaware, Newark (Master's thesis, advisor: K. Bischoff)
Freedson P, Katch VL, Sady S, Weltman A (1979) Cardiac output differences in males and females during mild cycle ergometer exercise. Med Sci Sports 11(1):16–19
Frey N, Laveille C, Paraire M, Francillard M, Holford NH, Jochemsen R (2003) Population PKPD modelling of the long-term hypoglycaemic effect of gliclazide given as a once-a-day modified release (MR) formulation. Br J Clin Pharmacol 55(2):147–157
Fuller LM, Banker FL, Butler JJ, Gamble JF, Sullivan MP (1975) The natural history of non-Hodgkin's lymphomata stages I and II. Br J Cancer Suppl 2:270–285
Gabrielsson J, Weiner D (2007) Pharmacokinetic and pharmacodynamic data analysis: concepts and applications, Fourth edn. Swedish Pharmaceutical Press
Gall MA, Nielsen FS, Smidt UM, Parving HH (1993) The course of kidney function in type 2 (non-insulin-dependent) diabetic patients with diabetic nephropathy. Diabetologia 36(10):1071–1078
Gerlowski LE, Jain RK (1983) Physiologically based pharmacokinetic modeling: principles and applications. J Pharm Sci 72(10):1103–1127
Gibaldi M, Perrier D (1999) Pharmacokinetics: revised and expanded. Drugs Pharma Sci 92:15–15
Gomeni R, Teneggi V, Iavarone L, Squassante L, Bye A (2001) Population pharmacokinetic-pharmacodynamic model of craving in an enforced smoking cessation population: indirect response and probabilistic modeling. Pharma Res 18(4):537–543
Grantham JJ, Cook LT, Torres VE, Bost JE, Chapman AB, Harris PC et al (2008) Determinants of renal volume in autosomal-dominant polycystic kidney disease. Kidney Int 73(1):108–116
Grehant N (1904a) Mesure de l'activite physio-logique des reins par le dosage de l'ure'e dans le sang et dans l'urine. J Physiol et Path Gen 7:1
Grehant N (1904b) Physiologique des reins par le dosage de l'uree dans le sang et daus l'urine. J physiol (Paris) 6:1–8
Gupta SK, Sathyan G, Lindemulder EA, Ho PL, Sheiner LB, Aarons L (1999) Quantitative characterization of therapeutic index: application of mixed-effects modeling to evaluate oxybutynin dose-efficacy and dose-side effect relationships. Clin Pharmacol Ther 65(6):672–684
Guyton AC, Hall JE (1996) Textbook of medical physiology, 9th edn. Saunders, Philadelphia
Hall JE, Guyton AC (2011) Guyton and hall textbook of medical physiology, 12th edn. Saunders, Philadelphia
Hamren B, Bjork E, Sunzel M, Karlsson M (2008) Models for plasma glucose, HbA1c, and hemoglobin interrelationships in patients with type 2 diabetes following tesaglitazar treatment. Clin Pharmacol Ther 84(2):228–235
Harrell FE (2001) Regression modeling strategies: with applications to linear models, logistic regression, and survival analysis, edn. Springer
Heiberger RM, Holland B (2004) Statistical analysis and data display: an intermediate course with examples in S-plus, R, and SAS, edn. Springer
Herman WH (2003) Diabetes modeling. Diabetes Care 26(11):3182–3183
Holford N (2013) A time to event tutorial for pharmacometricians. CPT Pharmacometrics Syst Pharmacol 2:e43
Holford NH, Peace KE (1992a) Methodologic aspects of a population pharmacodynamic model for cognitive effects in Alzheimer patients treated with tacrine. Proc Natl Acad Sci U S A 89(23):11466–11470
Holford NH, Peace KE (1992b) Results and validation of a population pharmacodynamic model for cognitive effects in Alzheimer patients treated with tacrine. Proc Natl Acad Sci U S A 89(23):11471–11475
Holford N, Ma SC, Ploeger BA (2010) Clinical trial simulation: a review. Clin Pharmacol Ther 88(2):166–182
Hougaard P (1995) Frailty models for survival data. Lifetime Data Anal 1(3):255–273

Hu TM, Hayton WL (2001) Allometric scaling of xenobiotic clearance: uncertainty versus universality. AAPS PharmSci 3(4):E29

Huang SM (2012) PBPK as a tool in regulatory review. Biopharm Drug Dispos 33(2):51–52

Huang SM, Rowland M (2012) The role of physiologically based pharmacokinetic modeling in regulatory review. Clin Pharmacol Ther 91(3):542–549

Hutter JC, Luu HM, Mehlhaff PM, Killam AL, Dittrich HC (1999) Physiologically based pharmacokinetic model for fluorocarbon elimination after the administration of an octafluoropropane-albumin microsphere sonographic contrast agent. J Ultrasound Med 18(1):1–11

Johnston SR, Hickish T, Ellis P, Houston S, Kelland L, Dowsett M et al (2003) Phase II study of the efficacy and tolerability of two dosing regimens of the farnesyl transferase inhibitor, R115777, in advanced breast cancer. J Clin Oncol 21(13):2492–2499

Jusko WJ, Ko HC (1994) Physiologic indirect response models characterize diverse types of pharmacodynamic effects. Clin Pharmacol Ther 56(4):406–419

Karlsson MO, Schoemaker RC, Kemp B, Cohen AF, van Gerven JM, Tuk B et al (2000) A pharmacodynamic Markov mixed-effects model for the effect of temazepam on sleep. Clin Pharmacol Ther 68(2):175–188

Kemp B, Kamphuisen HA (1986) Simulation of human hypnograms using a Markov chain model. Sleep 9(3):405–414

Kimko HC, Peck CC (2011) Clinical trial simulations: applications and trends, edn. Springer, New York

Kimko HC, Reele SS, Holford NH, Peck CC (2000) Prediction of the outcome of a phase 3 clinical trial of an antischizophrenic agent (quetiapine fumarate) by simulation with a population pharmacokinetic and pharmacodynamic model. Clin Pharmacol Ther 68(5):568–577

Kjellsson MC, Zingmark PH, Jonsson EN, Karlsson MO (2008) Comparison of proportional and differential odds models for mixed-effects analysis of categorical data. J Pharmacokinet Pharmacodyn 35(5):483–501

Knibbe CA, Zuideveld KP, DeJongh J, Kuks PF, Aarts LP, Danhof M (2002) Population pharmacokinetic and pharmacodynamic modeling of propofol for long-term sedation in critically ill patients: a comparison between propofol 6% and propofol 1%. Clin Pharmacol Ther 72(6):670–684

Kowalski KG, Hutmacher MM (2001) Design evaluation for a population pharmacokinetic study using clinical trial simulations: a case study. Stat Med 20(1):75–91

Kowalski KG, McFadyen L, Hutmacher MM, Frame B, Miller R (2003) A two-part mixture model for longitudinal adverse event severity data. J Pharmacokinet Pharmacodyn 30(5):315–336

Lacroix BD, Lovern MR, Stockis A, Sargentini-Maier ML, Karlsson MO, Friberg LE (2009) A pharmacodynamic Markov mixed-effects model for determining the effect of exposure to certolizumab pegol on the ACR20 score in patients with rheumatoid arthritis. Clin Pharmacol Ther 86(4):387–395

Landersdorfer CB, Jusko WJ (2008) Pharmacokinetic/pharmacodynamic modelling in diabetes mellitus. Clin Pharmacokinet 47(7):417–448

Lee PI (2001) Design and power of a population pharmacokinetic study. Pharma Res 18(1):75–82

Leong R, Vieira ML, Zhao P, Mulugeta Y, Lee CS, Huang SM et al (2012) Regulatory experience with physiologically based pharmacokinetic modeling for pediatric drug trials. Clin Pharmacol Ther 91(5):926–931

Lewis AE (1948) The concept of hepatic clearance. Am J Clin Pathol 18(10):789–795

Lewis EJ, Hunsicker LG, Bain RP, Rohde RD (1993) The effect of angiotensin-converting-enzyme inhibition on diabetic nephropathy. The Collaborative Study Group. N Engl J Med 329(20):1456–1462

Liu X, Smith BJ, Chen C, Callegari E, Becker SL, Chen X et al (2005) Use of a physiologically based pharmacokinetic model to study the time to reach brain equilibrium: an experimental analysis of the role of blood-brain barrier permeability, plasma protein binding, and brain tissue binding. J Pharmacol Exp Ther 313(3):1254–1262

Lunn DJ, Wakefield J, Racine-Poon A (2001) Cumulative logit models for ordinal data: a case study involving allergic rhinitis severity scores. Stat Med 20(15):2261–2285

Mager DE, Abernethy DR, Egan JM, Elahi D (2004) Exendin-4 pharmacodynamics: insights from the hyperglycemic clamp technique. J Pharmacol Exp Ther 311(2):830–835
Maiwald T, Timmer J (2008) Dynamical modeling and multi-experiment fitting with PottersWheel. Bioinformatics 24(18):2037–2043
Mandema JW, Stanski DR (1996) Population pharmacodynamic model for ketorolac analgesia. Clin Pharmacol Ther 60(6):619–635
McCullagh P (1980) Regression models for ordinal data. J R Stat Soc B 42(2): 109–142
McDonagh CF, Huhalov A, Harms BD, Adams S, Paragas V, Oyama S et al (2012) Antitumor activity of a novel bispecific antibody that targets the ErbB2/ErbB3 oncogenic unit and inhibits heregulin-induced activation of ErbB3. Mol Cancer Ther 11(3):582–593
Meibohm B, Laer S, Panetta JC, Barrett JS (2005) Population pharmacokinetic studies in pediatrics: issues in design and analysis. AAPS J 7(2):E475–E487
Metcalfe C, Thompson SG (2007) Wei, Lin and Weissfeld's marginal analysis of multivariate failure time data: should it be applied to a recurrent events outcome? Stat Methods Med Res 16(2):103–122
Mordenti J, Chappell W (1989) The use of interspecies scaling in toxicokinetics. In: Yacobi A, Skelly JP, Batra V (eds) Toxicokinetics and new drug development, edn. Pergamon, New York, pp 42–96
Mould D, Chapelsky M, Aluri J, Swagzdis J, Samuels R, Granett J (2001) A population pharmacokinetic-pharmacodynamic and logistic regression analysis of lotrafiban in patients. Clin Pharmacol Ther 69(4):210–222
Mould DR (2007) Developing models of disease progression. In: Ette EI, Williams PJ (eds) Pharmacometrics: the science of quantitative pharmacology, edn. Wiley, Hoboken, pp 547–581
Mould DR, Holford NH, Schellens JH, Beijnen JH, Hutson PR, Rosing H et al (2002) Population pharmacokinetic and adverse event analysis of topotecan in patients with solid tumors. Clin Pharmacol Ther 71(5):334–348
Mould DR, Denman NG, Duffull S (2007) Using disease progression models as a tool to detect drug effect. Clin Pharmacol Ther 82(1):81–86
Nestorov IA, Aarons LJ, Arundel PA, Rowland M (1998) Lumping of whole-body physiologically based pharmacokinetic models. J Pharmacokinet Biopharma 26(1):21–46
Nielsen EI, Friberg LE (2013) Pharmacokinetic-pharmacodynamic modeling of antibacterial drugs. Pharmacol Rev 65(3):1053–1090
Ogungbenro K, Aarons L (2008) How many subjects are necessary for population pharmacokinetic experiments? Confidence interval approach. Eur J Clin Pharmacol 64(7):705–713
Oliver RE, Jones AF, Rowland M (2001) A whole-body physiologically based pharmacokinetic model incorporating dispersion concepts: short and long time characteristics. J Pharmacokinet Pharmacodyn 28(1):27–55
Olofsen E, Romberg R, Bijl H, Mooren R, Engbers F, Kest B et al (2005) Alfentanil and placebo analgesia: no sex differences detected in models of experimental pain. Anesthesiology 103(1):130–139
Ouellet D, Sutherland S, Wang T, Griffini P, Murthy V (2011) First-time-in-human study with GSK1018921, a selective GlyT1 inhibitor: relationship between exposure and dizziness. Clin Pharmacol Ther 90(4):597–604
Pacini G, Bergman RN (1986) MINMOD: a computer program to calculate insulin sensitivity and pancreatic responsivity from the frequently sampled intravenous glucose tolerance test. Compute Methods Programs Biomed 23(2):113–122
Pang KS, Durk MR (2010) Physiologically-based pharmacokinetic modeling for absorption, transport, metabolism and excretion. J Pharmacokinet Pharmacodyn 37(6):591–615
Parving HH, Rossing P, Hommel E, Smidt UM (1995) Angiotensin-converting enzyme inhibition in diabetic nephropathy: ten years' experience. Am J Kidney Dis 26(1):99–107
Peters RH (1986) The ecological implications of body size, edn, Cambridge University Press
Peters SA (2008) Evaluation of a generic physiologically based pharmacokinetic model for lineshape analysis. Clin Pharmacokinet 47(4):261–275

Peters SA (2012) Physiologically-based pharmacokinetic (PBPK) modeling and simulations: principles, methods, and applications in the pharmaceutical industry, First edn. Wiley
Peters SA, Hultin L (2008) Early identification of drug-induced impairment of gastric emptying through physiologically based pharmacokinetic (PBPK) simulation of plasma concentration-time profiles in rat. J Pharmacokinet Pharmacodyn 35(1):1–30
Peterson B, Harrell Jr FE (1990) Partial proportional odds models for ordinal response variables. Appl Stat 39(2): 205–217
Pillai G, Gieschke R, Goggin T, Jacqmin P, Schimmer RC, Steimer JL (2004) A semimechanistic and mechanistic population PK-PD model for biomarker response to ibandronate, a new bisphosphonate for the treatment of osteoporosis. Br J Clin Pharmacol 58(6):618–631
Pors Nielsen S, Barenholdt O, Hermansen F, Munk-Jensen N (1994) Magnitude and pattern of skeletal response to long term continuous and cyclic sequential oestrogen/progestin treatment. Br J Obstet Gynaecol 101(4):319–324
Poulin P, Theil FP (2000) A priori prediction of tissue:plasma partition coefficients of drugs to facilitate the use of physiologically-based pharmacokinetic models in drug discovery. J Pharm Sci 89(1):16–35
Poulin P, Theil FP (2002a) Prediction of pharmacokinetics prior to in vivo studies. 1. Mechanism-based prediction of volume of distribution. J Pharm Sci 91(1):129–156
Poulin P, Theil FP (2002b) Prediction of pharmacokinetics prior to in vivo studies. II. Generic physiologically based pharmacokinetic models of drug disposition. J Pharm Sci 91(5):1358–1370
Poulin P, Schoenlein K, Theil FP (2001) Prediction of adipose tissue: plasma partition coefficients for structurally unrelated drugs. J Pharm Sci 90(4):436–447
Ramsey JC, Andersen ME (1984) A physiologically based description of the inhalation pharmacokinetics of styrene in rats and humans. Toxicol Appl Pharmacol 73(1):159–175
Ravva P, Gastonguay MR, Tensfeldt TG, Faessel HM (2009) Population pharmacokinetic analysis of varenicline in adult smokers. Br J Clin Pharmacol 68(5):669–681
Reddy M, Yang R, Andersen ME, Clewell III HJ (2005) Physiologically based pharmacokinetic modeling: science and applications, First edn. Wiley-Interscience
Rosch J, Antonovic R, Trenouth RS, Rahimtoola SH, Sim DN, Dotter CT (1976) The natural history of coronary artery stenosis. A longitudinal angiographic assessment. Radiology 119(3):513–520
Ross SM (2006) Introduction to probability models, edn. Access Online via Elsevier
Rowland M (1972) Application of clearance concepts to some literature data on drug metabolism in the isolated perfused liver preparation and in vivo. Eur J Pharmacol 17(3):352–356
Rowland M, Tozer TN (1989) Clinical pharmacokinetics: concepts and applications, edn, vol. 162. Lea & Febiger, Philadelphia
Rowland M, Benet LZ, Graham GG (1973) Clearance concepts in pharmacokinetics. J Pharmacokinet Biopharma 1(2):123–136
Rowland M, Peck C, Tucker G (2011) Physiologically-based pharmacokinetics in drug development and regulatory science. Annu Rev Pharmacol and Toxicol 51:45–73
Sadray S, Jonsson EN, Karlsson MO (1999) Likelihood-based diagnostics for influential individuals in non-linear mixed effects model selection. Pharm Res 16(8):1260–1265
Savage VM, Gillooly J, Woodruff W, West G, Allen A, Enquist B et al (2004) The predominance of quarter-power scaling in biology. Funct Ecol 18(2):257–282
Savic RM, Karlsson MO (2009) Importance of shrinkage in empirical bayes estimates for diagnostics: problems and solutions. AAPS J 11(3):558–569
Schmidt S, Post TM, Boroujerdi MA, van Kesteren C, Ploeger BA, Della Pasqua OE et al (2011) Disease progression analysis: towards mechanism-based models. In: Kimko HC, Peck CC (eds) Clinical trial simulations, edn. Springer, New York, pp 433–455
Schoeberl B, Pace EA, Fitzgerald JB, Harms BD, Xu L, Nie L et al (2009) Therapeutically targeting ErbB3: a key node in ligand-induced activation of the ErbB receptor-PI3K axis. Sci Signal 2(77):ra31
Sheiner LB, Ludden TM (1992) Population pharmacokinetics/dynamics. Annu Rev Pharmacol Toxicol 32:185–209

Sheiner LB, Rosenberg B, Marathe VV (1977) Estimation of population characteristics of pharmacokinetic parameters from routine clinical data. J Pharmacokinet Biopharma 5(5):445–479
Sheiner LB, Stanski DR, Vozeh S, Miller RD, Ham J (1979) Simultaneous modeling of pharmacokinetics and pharmacodynamics: application to d-tubocurarine. Clin Pharmacol Ther 25(3):358–371
Sy SK, Heuberger J, Shilbayeh S, Conrado DJ, Derendorf H (2013a) A Markov Chain model to evaluate the effect of CYP3A5 and ABCB1 polymorphisms on adverse events associated with tacrolimus in pediatric renal transplantation. AAPS J 15(4):1189–99
Sy SK, Singh RP, Shilbayeh S, Zmeili R, Conrado D, Derendorf H (2013b) Influence of CYP3A5 6986A > G and ABCB1 3435C > T Polymorphisms on Adverse Events Associated With Tacrolimus in Jordanian Pediatric Renal Transplant Patients. Clin Pharmacol Drug Dev 2(1):67–78
Teorell T (1937a) Kinetics of distribution of substances administered to the body, I: the extravascular modes of administration. Arch Int pharmacodyn Ther 57:205–225
Teorell T (1937b) Kinetics of distribution of substances administered to the body, II: the intravascular modes of administration. Arch Int Pharmacodyn Ther 57:226–240
Theil FP, Guentert TW, Haddad S, Poulin P (2003) Utility of physiologically based pharmacokinetic models to drug development and rational drug discovery candidate selection. Toxicol Lett 138(1–2):29–49
Thomaseth K, Salvan A (1998) Estimation of occupational exposure to 2,3,7,8-tetrachlorodibenzo-p-dioxin using a minimal physiologic toxicokinetic model. Environ Health Perspect 106(Suppl 2):743–753
Troconiz IF, Plan EL, Miller R, Karlsson MO (2009) Modelling overdispersion and Markovian features in count data. J Pharmacokinet Pharmacodyn 36(5):461–477
U.S. Department of Health and Human Services, Food and Drug Administration. DA (1999) Guidance for industry: population pharmacokinetics, (available at http://www.fda.gov/downloads/ScienceResearch/SpecialTopics/WomensHealthResearch/UCM133184.pdf)
van der Molen GW, Kooijman SA, Slob W (1996) A generic toxicokinetic model for persistent lipophilic compounds in humans: an application to TCDD. Fundam Appl Toxicol 31(1):83–94
Venables WN, Ripley BD, Venables W (1994) Modern applied statistics with S-PLUS, edn, vol. 250. Springer, New York
Vong C, Bergstrand M, Nyberg J, Karlsson MO (2012) Rapid sample size calculations for a defined likelihood ratio test-based power in mixed-effects models. AAPS J 14(2):176–186
Wada DR, Bjorkman S, Ebling WF, Harashima H, Harapat SR, Stanski DR (1997) Computer simulation of the effects of alterations in blood flows and body composition on thiopental pharmacokinetics in humans. Anesthesiology 87(4):884–899
Wang X, Santostefano MJ, Evans MV, Richardson VM, Diliberto JJ, Birnbaum LS (1997) Determination of parameters responsible for pharmacokinetic behavior of TCDD in female Sprague-Dawley rats. Toxicol Appl Pharmacol 147(1):151–168
Wei L, Glidden DV (1997) An overview of statistical methods for multiple failure time data in clinical trials. Stat Med 16(8):833–839
Wei L-J, Lin DY, Weissfeld L (1989) Regression analysis of multivariate incomplete failure time data by modeling marginal distributions. J Am Stat Assoc 84(408):1065–1073
West GB, Brown JH, Enquist BJ (1997) A general model for the origin of allometric scaling laws in biology. Science 276(5309):122–126
West GB, Brown JH, Enquist BJ (1999) The fourth dimension of life: fractal geometry and allometric scaling of organisms. Science 284(5420):1677–1679
Wilkinson GR (1987) Clearance approaches in pharmacology. Pharmacol Rev 39(1):1–47
Wilkinson GR, Shand DG (1975) Commentary: a physiological approach to hepatic drug clearance. Clin Pharmacol Ther 18(4):377–390
Xie R, Mathijssen RH, Sparreboom A, Verweij J, Karlsson MO (2002) Clinical pharmacokinetics of irinotecan and its metabolites in relation with diarrhea. Clin Pharmacol Ther 72(3):265–275
Yamaoka K, Nakagawa T, Uno T (1978) Statistical moments in pharmacokinetics. J Pharmacokinet Biopharma 6(6):547–558

Yang J, Zhao H, Garnett C, Rahman A, Gobburu JV, Pierce W et al (2012) The combination of exposure-response and case-control analyses in regulatory decision making. J Clin Pharmacol 53(2):160–6

Yim DS, Zhou H, Buckwalter M, Nestorov I, Peck CC, Lee H (2005) Population pharmacokinetic analysis and simulation of the time-concentration profile of etanercept in pediatric patients with juvenile rheumatoid arthritis. J Clin Pharmacol 45(3):246–256

Zhao W, Elie V, Roussey G, Brochard K, Niaudet P, Leroy V et al (2009) Population pharmacokinetics and pharmacogenetics of tacrolimus in de novo pediatric kidney transplant recipients. Clin Pharmacol Ther 86(6):609–618

Zhao P, Zhang L, Grillo JA, Liu Q, Bullock JM, Moon YJ et al (2011) Applications of physiologically based pharmacokinetic (PBPK) modeling and simulation during regulatory review. Clin Pharmacol Ther 89(2):259–267

Zhao P, Rowland M, Huang SM (2012) Best practice in the use of physiologically based pharmacokinetic modeling and simulation to address clinical pharmacology regulatory questions. Clin Pharmacol Ther 92(1):17–20

Zingmark PH, Ekblom M, Odergren T, Ashwood T, Lyden P, Karlsson MO et al (2003) Population pharmacokinetics of clomethiazole and its effect on the natural course of sedation in acute stroke patients. Br J Clin Pharmacol 56(2):173–183